Nonlocal Third-order shear deformation theory for analysis of laminated plates considering surface stress effects

P. Raghu[1], K. Preethi[1], A. Rajagopal[1*], and J. N. Reddy[2]

[1]Department of Civil Engineering , IIT Hyderabad, India
[2]Department of Mechanical Engineering, Texas A&M University, College Station, Texas, USA

Abstract

In this work, we present analytical solutions for laminated composite plates using a nonlocal third-order shear deformation theory considering the surface stress effects. The theory is based on Eringen's theory of nonlocal continuum mechanics [1] and the third-order plate theory of Reddy [2]. The mathematical formulation for surface stress is based on Gurtin and Murdoch's work [3],[4]. In the nonlocal theory we consider the size effect by assuming that the stress at a point depends on the strain at that point as well as on the strains at the neighboring points. Analytical solutions of bending and vibration of a simply supported laminates and isotropic plates are presented using this theory to illustrate the effect of nonlocality and surface stress on deflection and vibration frequencies for various span-to-thickness (a/h) ratios.

1 Introduction

In modeling micro and nano structures, where the size effect is prominent (e.g., study of elastic waves when dispersion effect is taken to account and the determination of stress at the crack tip when the singularity of the solution is of concern), conventional theories cannot model the material behavior accurately. There has been considerable focus towards the development of generalized continuum theories which account for the inherent micro-structure in natural and engineering materials (see [5], [6], [7], and [8]). The notion of

generalized continua unifies several extended continuum theories that account for such size dependence due to the underlying micro-structure of the material. A systematic overview and detailed discussion of generalized continuum theories has been given by Bazant and Jirasek [9]. These theories can be categorized as gradient continuum theories (see the works by Mindilin et al. [10], [11], [12], Toupin[13], Steinmann et al. [6], [14], [15], [16], Casterzene et al. [17], Fleck et al. [18], [19], Askes et al. [20], [21], [22]), micro continuum theories (see Eringen [23], [24], [5], [25], [1], Steinmann et al. [26], [27]), and nonlocal continuum theories (see works by Eringen [25], Jirasek [28], [29], Reddy [30], [31], [32], [33] and others [34]). Recently, the higher-order gradient theory for finite deformation has been elaborated (for instance see [35], [36], [37], [17], and [38]), within classical continuum mechanics in the context of homogenization approaches. A comparison of various higher-order gradient theories can be found in [18]. A more detailed formulation of gradient approach in spatial and material setting has been presented in [26].

Nonlocality of the stress-strain relationship introduces length scale at which classical elasticity theories break down. Classical theory is inherently size independent. The nonlocal formulations can be of integral-type formulations with weighted spatial averaging or by implicit gradient models which are categorized as strongly nonlocal, while weakly nonlocal theories include for instance explicit gradient models [9]. The nonlocality arises due to the discrete structure of matter and the fluctuations in the inter-atomic forces. The two dominant physical mechanisms that lead to size dependency of elastic behavior at the nanoscale are surface energy effects and nonlocal interactions [39]. Recently, various beam theories (e.g., Euler-Bernoulli, Timoshenko, Reddy, and Levinson beam theories) were reformulated using Eringen's nonlocal differential constitutive model by Reddy [30]. The analytical solutions for bending, buckling, and natural vibrations for isotropic plates were also presented in [30]. Various shear deformation beam theories were also reformulated in recent works by Reddy [30] using nonlocal differential constitutive relations. Similar works have been carried out by Aydogdu [31] and Civalek [32].

Nonlocal elastic rod models have been developed to investigate the small-scale effect on axial vibrations of the nanorods by Aydogdu [40] and Adhikari et al. [41]. Free vibration analysis of microtubules based on nonlocal theory and Euler-Bernoulli beam theory was done by Civalek et al. [32]. Free vibration analysis of functionally graded carbon nanotube with various thickness based on Timoshenko beam theory has been investigated to obtain numerical solutions using the Differential Quadrature Method (DQM) by Janghorban et al. [42] and others (see [43], [44] & [45]). Eringen's nonlocal elasticity theory has also been applied to study bending, buckling, and vibration of nanobeams using the Timoshenko beam theory (see [46], [47], [48] and [49]). Numerical solutions were obtained by a meshless method. Two different collocation techniques, global (RDF) and local (RDF-FD), were used with multi-quadrics radial basis functions by Roque et al. [50]. Static deformation of micro- and

nano-structures were studied using nonlocal Euler-Bernoulli and Timoshenko beam theories and explicit solutions were derived for displacements for standard boundary conditions by Wang et al. [51, 52, 53]. Iterative nonlocal elasticity for Kirchhoff plates has been presented in [54]. Thai et al. [55] developed a nonlocal shear deformation beam theory with a higher-order displacement field that does not require shear correction factors [56]. Analytical study on the nonlinear free vibration of functionally graded nanobeams incorporating surface effects has been presented in [57], [58] and [59]. The effect of nonlocal parameter, surface elasticity modulus, and residual surface stress on the vibrational frequencies of Timoshenko beam has been studied in [60] and [61]. The coupling between nonlocal effect and surface stress effect for the nonlinear free vibration case of nanobeams has been studied in [62].

Some explicit solutions involving trigonometric expansions are also presented recently for nonlocal analysis of beams [63]. A finite element framework for nonlocal analysis of beams is presented in a recent work by Sciarra et al.[64]. Size effects on elastic moduli of plate like nanomaterials has been studied in [65]. Studies to understand thermal vibration of single wall carbon nanotube embedded in an elastic medium using DQM has also been reported in [66]. The recent studies has been towards the application of nonlocal nonlinear formulations for the vibration analysis of functionally graded beams [67]. The effect of surface stresses on bending properties of metal nanowires is presented in [68]. There has been some works on transforming nonlocal approaches to gradient type formulations [69]. Semi analytical approach for large amplitude free vibration and buckling of nonlocal functionally graded beams has been reported in [70]. Barretta et al. [71] derived a new variational frame work following the gradient type nonlocal constitutive law and a thermodynamic approach. Wang et al. [51] presented the scale effect on static deformation of micro- and nano-rods or tubes through nonlocal EulerBernoulli beam theory and Timoshenko beam theory. Explicit solutions for static deformation of such structures with standard boundary conditions are derived. Huu et al.[55] based on the modified couple stress theory and Timoshenko beam theory examined static bending ,buckling and free vibration behaviors of size dependent functionally graded sandwich micro beams [56].

These nonlocal laminated plate theories allow for the small-scale effect which becomes significant when dealing with micro and nano laminated plate-like structures [30]. The nonlocality arises due to the discrete structure of matter and the fluctuations in the inter atomic forces [72]. In the case of plate like structures, when the width to thickness ratio of the plate becomes less than 20, transverse shear stresses play a key role on the behaviour of the plate. Various theories have been developed to take care of shear strains into account such as first order shear deformation theory (FSDT) by Mindlin, Third order shear deformation theory (TSDT) by Reddy [2], and other generalized higher order shear deformation theories (e.g., see [73], [74], [75], [76], [77], [78], and [79]). Lu et al. [80] proposed a non-local plate model based on Eringens theory of nonlocal continuum mechanics. The basic equations for

the non-local Kirchhoff and the Mindlin plate theories are derived. Maranganti et al. [39] estimated nonlocal elasticity length scales for various classes of materials like semiconductors, metals, amorphous solids, and polymers using a combination of empirical molecular dynamics and lattice dynamics. The effect of inter atomic forces is also studied. Farajpoura et al. [81] investigated the buckling response of orthotropic single layered graphene sheet subjected to linearly varying normal stresses using the nonlocal elasticity theory. The nonlocal theory of Eringen and the equilibrium equations of a rectangular plate are employed to derive the governing equations. Differential quadrature method (DQM) has been used to solve the governing equations for various boundary conditions.

Wang et al.[79] presented a large-deflection mathematical analysis of rectangular plates under uniform lateral loading. The analysis is based on solving two fourth-order, second-degree, partial differential Von Krmn equations relating the lateral deflections to the applied load. Plates with two boundary conditions, namely, simply supported edges and held edges, are considered. Neves et al. [82] derived higher-order shear deformation theory for modeling functionally graded plates to account for extensibility in the thickness direction. Arash et al. [83] studied the application of the nonlocal continuum theory in modeling of carbon nano tubes and graphene sheets. A variety of nonlocal continuum models in modeling of the two materials under static and dynamic loadings are introduced and reviewed. The superiority of nonlocal continuum models to their local counterparts, the necessity of the calibration of the small-scale parameter, and the applicability of nonlocal continuum models are discussed. Yan et al. [84] applied nonlocal continuum mechanics to derive complete and asymptotic representation of the infinite higher-order governing differential equations for nano-beam and nano-plate models. Wang et al. [85] presented elastic buckling analysis of micro- and nano-rods/tubes based on Eringens nonlocal elasticity theory and the Timoshenko beam theory. Sun et al. [65] presented a semi continuum model for nano structured materials that possess a plate like geometry such as ultra-thin films. This model accounts for the discrete nature in the thickness direction. In-plane Youngs modulus, and in-plane and out-plane Poissons ratios are investigated with this model. It is found that the values of the Youngs modulus and Poissons ratios depend on the number of atomic layers in the thickness direction and approach the respective bulk values as the number of atom layers increases. Murmu et al. [86] solved vibration of double-nano beam-systems which are important in nano-optomechanical systems and sensor applications. Expressions for free bending-vibration of double-nano beam-system are established within the framework of Eringens nonlocal elasticity theory. The increase in the stiffness of the coupling springs in double-nano beam-system reduces the nonlocal effects during the out-of-phase modes of vibration. Wang et al. [87] conducted study of the mechanisms of nonlocal effect on the transverse vibration of two-dimensional 2D nano plates, for example, mono layer graphene and boron-nitride sheets. It is found that such a nonlocal effect stems from a distributed transverse force due to the curvature change in the nanoplates

and the surface stress due to the nonlocal atom-to-atom interaction. Using the principle of virtual work the governing equations are derived for rectangular nanoplates. Solutions for buckling loads are computed using differential quadrature method (DQM). It is shown that the nonlocal effect is quite significant in graphene sheets and has a decreasing effect on the buckling loads. Murmu et al. (see [88],[89], and [90]) have studied small-scale effects on the free in-plane vibration of nano plates are investigated employing nonlocal continuum mechanics. Equations of motion of the nonlocal plate model for this study are derived and presented. Explicit relations for natural frequencies are obtained through direct separation of variables. It has been shown that nonlocal effects are quite significant in in-plane vibration studies and need to be included in the continuum model of nanoplates such as in graphene sheets. Han et al. [91] studied influence of the molecular structure on indentation size effect in polymers. The indentation size effect in polymers is examined which manifests itself in increased hardness at decreasing indentation depths. Nikolov et al. [92] applied the micro-mechanical origin of size effects in elasticity of solid polymers. It was shown that size effects related to rotational gradients can be interpreted in terms of Frank elasticity arising from the finite bending stiffness of the polymer chains and their interactions. A relationship between the gradient of the nematic director field, related to the orientation of the polymer segments, and the curvature tensor associated with rotational gradients was derived.

The focus of the present work is to develop analytical solutions for bending and free vibration of laminates composite plates using the nonlocal third-order shear deformation theory which accounts for surface stress effects. The solutions using nonlocal theories are based on Eringen's theory of nonlocal continuum mechanics [1]. The nonlocal theory considers the size effect by assuming that stress at a point depends on the strain not only at that point but also on the neighbouring points. Analytical solutions of bending and vibration of a simply supported rectangular laminates are presented using this theory to illustrate the effect of nonlocality on deflection and free vibration for various a/h and a/b ratios. The paper is organized as below in Section 2 we present the introduction to nonlocal theories. In Section 3 the third order shear deformation theory with nonlocal and surface effects is presented. The surface stresses for plates and laminates are discussed in detail in this section. The equilibrium equations are also presented in the section. In Section 4 we present analytical solutions for various types of laminates. Lastly, Section 5 is devoted to numerical examples.

2 Nonlocal theories

Nonlocal elasticity theory invokes the length scale parameter in order to account for the size effects [1]. Neglecting the size effects, when dealing with micro and nano scale fields, may result in inaccurate solution and hence resulting in wrong designs. So one must consider the small scale effects and atomic forces to obtain the solutions with acceptable accuracy.

In nonlocal elasticity theory, it is assumed that the stress at a point in a continuum body is function of the strain at all neighbor points of the continuum, hence the effects of small scale and atomic forces are considered as material parameters in the constitutive equation. Following experimental observations, Eringen proposed a constitutive model that expresses the nonlocal stress tensor $\boldsymbol{\sigma}^{nl}$ at point x as

$$\boldsymbol{\sigma}^{nl} = \int K(|\boldsymbol{x}' - \boldsymbol{x}|, \tau)\boldsymbol{\sigma}(\boldsymbol{x}')\, dx' \tag{1}$$

where, $\boldsymbol{\sigma}(x)$ is the classical macroscopic stress tensor at point x and $K(|\boldsymbol{x}' - \boldsymbol{x}|, \tau)$ is the Kernel function which is normalized over the volume of the body represents the nonlocal modulus. $|\boldsymbol{x}' - \boldsymbol{x}|$ is the nonlocal distance and τ is the material constant that depends on the internal and external characteristic length.

As per Hooke's law we have

$$\boldsymbol{\sigma}(\boldsymbol{x}) = \boldsymbol{C}(\boldsymbol{x}) : \boldsymbol{\epsilon}(\boldsymbol{x}) \tag{2}$$

where $\boldsymbol{\varepsilon}$ is the strain tensor and $\boldsymbol{C}$ is the fourth-order elasticity tensor. Equations (1) and (2) together form the nonlocal constitutive equation for Hookean solid. Equation (1) can be represented equivalently in differential form as

$$\left(1 - \tau^2 l^2 \nabla^2\right) \boldsymbol{\sigma}^{nl} = \boldsymbol{\sigma} \tag{3}$$

where $\tau = \frac{(e_0 a)^2}{l^2}$, e_0 is a material constant and a and l are the internal and external characteristic lengths respectively. In general, ∇^2 is the three-dimensional Laplace operator. The nonlocal parameter μ can be taken as $\mu = \tau^2 l^2$.

3 Third-order shear deformation theory

In the third-order shear deformation theory (TSDT) of Reddy [93] the assumptions of straightness and normality of the transverse normal after deformation are relaxed by expanding the displacements as cubic functions of thickness coordinate. Consequently, the transverse shear strains and transverse shear stresses vary quadratically through the thickness of the laminate and avoids the need for shear correction factors. Here the Reddy third-order shear deformation theory is reformulated to account for the surface stress effect.

3.1 Displacement field

The displacement field is based on a quadratic variation of transverse shear strains (and hence stresses) and vanishing of transverse shear stresses on top and bottom of a general laminate

composed of different layers. The displacement field of the Reddy third-order theory [93, 2] is

$$\begin{aligned} u(x,y,z) &= u_0(x,y) + z\phi_x - \frac{4z^3}{3h^2}\left(\phi_x + \frac{\partial w_0}{\partial x}\right) \\ v(x,y,z) &= v_0(x,y) + z\phi_y - \frac{4z^3}{3h^2}\left(\phi_y + \frac{\partial w_0}{\partial y}\right) \\ w(x,y,z) &= w_0(x,y) \end{aligned} \tag{4}$$

where u_0, v_0, w_0 are in-plane displacements of a point on the mid-plane (i.e., $z = 0$). ϕ_x and ϕ_y denote the rotations of a transverse normal line at the mid-plane ($\phi_x = \frac{\partial u}{\partial z}$ and $\phi_y = \frac{\partial u}{\partial z}$). The total thickness of the laminate is given by h.

3.2 Strain-displacement relations

The strain fields of the TSDT is

$$\begin{Bmatrix} \varepsilon_{xx} \\ \varepsilon_{yy} \\ \gamma_{xy} \end{Bmatrix} = \begin{Bmatrix} \varepsilon_{xx}^{(0)} \\ \varepsilon_{yy}^{(0)} \\ \gamma_{xy}^{(0)} \end{Bmatrix} + z \begin{Bmatrix} \varepsilon_{xx}^{(1)} \\ \varepsilon_{yy}^{(1)} \\ \gamma_{xy}^{(1)} \end{Bmatrix} + z^3 \begin{Bmatrix} \varepsilon_{xx}^{(3)} \\ \varepsilon_{yy}^{(3)} \\ \gamma_{xy}^{(3)} \end{Bmatrix} \tag{5}$$

$$\begin{Bmatrix} \gamma_{yz} \\ \gamma_{xz} \end{Bmatrix} = \begin{Bmatrix} \gamma_{yz}^{(0)} \\ \gamma_{xz}^{(0)} \end{Bmatrix} + z^2 \begin{Bmatrix} \gamma_{yz}^{(2)} \\ \gamma_{xz}^{(2)} \end{Bmatrix} \tag{6}$$

where

$$\begin{Bmatrix} \varepsilon_{xx}^{(0)} \\ \varepsilon_{yy}^{(0)} \\ \gamma_{xy}^{(0)} \end{Bmatrix} = \begin{Bmatrix} \frac{\partial u_0}{\partial x} \\ \frac{\partial v_0}{\partial y} \\ \frac{\partial u_0}{\partial y} + \frac{\partial v_0}{\partial x} \end{Bmatrix}, \quad \begin{Bmatrix} \varepsilon_{xx}^{(1)} \\ \varepsilon_{yy}^{(1)} \\ \gamma_{xy}^{(1)} \end{Bmatrix} = \begin{Bmatrix} \frac{\partial \phi_x}{\partial x} \\ \frac{\partial \phi_y}{\partial y} \\ \frac{\partial \phi_x}{\partial y} + \frac{\partial \phi_y}{\partial x} \end{Bmatrix} \tag{7}$$

$$\begin{Bmatrix} \varepsilon_{xx}^{(3)} \\ \varepsilon_{yy}^{(3)} \\ \gamma_{xy}^{(3)} \end{Bmatrix} = -c_1 \begin{Bmatrix} \frac{\partial \phi_x}{\partial x} + \frac{\partial^2 w_0}{\partial x^2} \\ \frac{\partial \phi_y}{\partial y} + \frac{\partial^2 w_0}{\partial y^2} \\ \frac{\partial \phi_x}{\partial y} + \frac{\partial \phi_y}{\partial x} + 2\frac{\partial^2 w_0}{\partial x \partial y} \end{Bmatrix} \tag{8}$$

$$\begin{Bmatrix} \gamma_{yz}^{(0)} \\ \gamma_{xz}^{(0)} \end{Bmatrix} = \begin{Bmatrix} \phi_y + \frac{\partial w_0}{\partial y} \\ \phi_x + \frac{\partial w_0}{\partial x} \end{Bmatrix}, \quad \begin{Bmatrix} \gamma_{yz}^{(2)} \\ \gamma_{xz}^{(2)} \end{Bmatrix} = -c_2 \begin{Bmatrix} \phi_y + \frac{\partial w_0}{\partial y} \\ \phi_x + \frac{\partial w_0}{\partial x} \end{Bmatrix} \tag{9}$$

where $c_1 = \frac{4}{3h^2}$ and $c_2 = 3c_1$.

3.3 Stress-strain relationships

The constitutive equations for each layer in the global coordinates are given by

$$\begin{Bmatrix}\sigma_{xx}\\ \sigma_{yy}\\ \sigma_{xy}\end{Bmatrix} = \begin{bmatrix}\bar{Q}_{11} & \bar{Q}_{12} & \bar{Q}_{16}\\ \bar{Q}_{12} & \bar{Q}_{22} & \bar{Q}_{26}\\ \bar{Q}_{16} & \bar{Q}_{26} & \bar{Q}_{66}\end{bmatrix} \begin{Bmatrix}\varepsilon_{xx}\\ \varepsilon_{yy}\\ \varepsilon_{xy}\end{Bmatrix}, \quad \begin{Bmatrix}\sigma_{yz}\\ \sigma_{xz}\end{Bmatrix} = \begin{bmatrix}\bar{Q}_{44} & \bar{Q}_{45}\\ \bar{Q}_{45} & \bar{Q}_{55}\end{bmatrix} \begin{Bmatrix}\gamma_{yz}\\ \gamma_{xz}\end{Bmatrix} \tag{10}$$

where

$$\begin{aligned}
\bar{Q}_{11} &= Q_{11}\left[\cos^4\theta + 2\left(Q_{12}+2Q_{66}\right)\sin^2\theta\cos^2\theta\right] + Q_{22}\sin^4\theta\\
\bar{Q}_{12} &= \left(Q_{11}+Q_{22}-4Q_{66}\right)\sin^2\theta\cos^2\theta + Q_{12}\left(\sin^4\theta+\cos^4\theta\right)\\
\bar{Q}_{16} &= \left(Q_{11}-Q_{12}-2Q_{66}\right)\sin\theta\cos^3\theta + \left(Q_{12}-Q_{22}+2Q_{66}\right)\sin^3\theta\cos\theta\\
\bar{Q}_{22} &= Q_{11}\sin^4\theta + 2\left(Q_{16}+2Q_{66}\right)\sin^2\theta\cos^2\theta + Q_{22}\cos^4\theta\\
\bar{Q}_{26} &= \left(Q_{11}-Q_{12}-2Q_{66}\right)\sin^3\theta\cos\theta + \left(Q_{12}-Q_{22}+2Q_{66}\right)\sin\theta\cos^3\theta\\
\bar{Q}_{66} &= \left(Q_{11}+Q_{22}-2Q_{12}-2Q66\right)\sin^2\theta\cos^2\theta + Q_{66}\sin^4\theta\cos^4\theta
\end{aligned} \tag{11}$$

$$\begin{aligned}
\bar{Q}_{44} &= Q_{44}\cos^2\theta + Q_{55}\sin^2\theta\\
\bar{Q}_{45} &= \left(Q_{55}-Q_{44}\right)\cos\theta\sin\theta\\
\bar{Q}_{55} &= Q_{44}\sin^2\theta + Q_{55}\cos^2\theta
\end{aligned} \tag{12}$$

$$Q_{11} = \frac{E_1}{1-\nu_{12}\nu_{21}}, \quad Q_{12} = \frac{\nu_{12}E_1}{1-\nu_{12}\nu_{21}}, \quad Q_{22} = \frac{E_2}{1-\nu_{12}\nu_{21}}, \quad Q_{66} = G_{12}, \tag{13}$$

$$Q_{16} = Q_{26} = 0, \quad Q_{44} = G_{23}, \quad Q_{45} = G_{12}, \quad Q_{55} = G_{13} \tag{14}$$

where θ is the orientation, measured in counterclockwise, from the fiber direction to the positive x-axis, E_1 and E_2 are elastic moduli, ν_{12} and ν_{21} are Poisson's ratios, and G_{12}, G_{13} and G_{23} are the shear moduli.

3.3.1 Surface stress

Because of interaction between the elastic surface and bulk material, in-plane forces in different directions act on the plate. The resulting in-plane loads lead to surface stresses. The general expression for surface stresses as given by Gurtin and Murdoch (see [3] and [4]) is given by

$$\sigma^s_{\alpha\beta} = \tau^s\delta_{\alpha\beta} + 2(\mu^s-\tau^s)\varepsilon_{\alpha\beta} + (\lambda^s+\tau^s)u_{\gamma,\gamma}\delta_{\alpha\beta} + \tau^s u_{\alpha,\beta} \tag{15a}$$

$$\sigma^s_{3\beta} = \tau^s u_{3,\beta} \tag{15b}$$

where $\alpha, \beta, \gamma = 1, 2$ and where λ^s and μ^s are the Lame's constants and τ^s is the surface stress parameter. From equations (15), we can write individual surface stresses as

$$\sigma^s_{xx} = (2\mu^s + \lambda^s - \tau^s)\,\varepsilon_{xx} + (\lambda^s + \tau^s)\,\varepsilon_{yy} + \left(1 + \frac{\partial u}{\partial x}\right)\tau^s \tag{16}$$

$$\sigma^s_{yy} = (2\mu^s + \lambda^s - \tau^s)\,\varepsilon_{yy} + (\lambda^s + \tau^s)\,\varepsilon_{xx} + \left(1 + \frac{\partial v}{\partial y}\right)\tau^s \tag{17}$$

$$\sigma^s_{xy} = 2\,(\mu^s - \tau^s)\,\varepsilon_{xy} + \tau^s \frac{\partial u}{\partial y} \tag{18}$$

$$\sigma^s_{xz} = \tau^s \frac{\partial w}{\partial x} \tag{19}$$

$$\sigma^s_{yz} = \tau^s \frac{\partial w}{\partial y} \tag{20}$$

Gurtin and Murdoch also gave the surface equilibrium equations as

$$\sigma^s_{i\alpha,\alpha} + \sigma_{i3} = \rho^s \ddot{u}_i \tag{21}$$

where $i = 1, 2, 3$ and $\alpha = 1, 2$. The equilibrium equation (21) will not be satisfied since we have taken σ_{zz} to be zero. To satisfy the equilibrium condition (21), we assume σ_{zz} to vary linearly through the thickness and is given by the equation

$$\begin{aligned}\sigma_{zz} = &\left[\frac{\left(\frac{\partial \sigma^s_{xz}}{\partial x} + \frac{\partial \sigma^s_{yz}}{\partial y} - \rho^s \frac{\partial w}{\partial t^2}\right)\Big|_{\text{at top}} + \left(\frac{\partial \sigma^s_{xz}}{\partial x} + \frac{\partial \sigma^s_{yz}}{\partial y} - \rho^s \frac{\partial w}{\partial t^2}\right)\Big|_{\text{at bottom}}}{2}\right] \\ &+ \left[\frac{\left(\frac{\partial \sigma^s_{xz}}{\partial x} + \frac{\partial \sigma^s_{yz}}{\partial y} - \rho^s \frac{\partial w}{\partial t^2}\right)\Big|_{\text{at top}} - \left(\frac{\partial \sigma^s_{xz}}{\partial x} + \frac{\partial \sigma^s_{yz}}{\partial y} - \rho^s \frac{\partial w}{\partial t^2}\right)\Big|_{\text{at bottom}}}{h}\right] z\end{aligned} \tag{22}$$

The superscript s is used to denote the quantities corresponding to the surface.

3.4 Stress resultants

The stress resultants for TSDT including surface stress effects are given as

$$\begin{Bmatrix} N_{xx} \\ N_{yy} \\ N_{xy} \end{Bmatrix} = \int_A \begin{Bmatrix} \sigma^k_{xx} \\ \sigma^k_{yy} \\ \sigma_{xy} \end{Bmatrix} dA + \oint_\Gamma \begin{Bmatrix} \sigma^s_{xx} \\ \sigma^s_{yy} \\ 0 \end{Bmatrix} dS \tag{23}$$

$$\begin{Bmatrix} M_{xx} \\ M_{yy} \\ M_{xy} \end{Bmatrix} = \int_A \begin{Bmatrix} \sigma^k_{xx} \\ \sigma^k_{yy} \\ \sigma_{xy} \end{Bmatrix} z\, dA + \oint_\Gamma \begin{Bmatrix} \sigma^s_{xx} \\ \sigma^s_{yy} \\ 0 \end{Bmatrix} z\, dS \tag{24}$$

$$\begin{Bmatrix} P_{xx} \\ P_{yy} \\ P_{xy} \end{Bmatrix} = \int_A \begin{Bmatrix} \sigma^k_{xx} \\ \sigma^k_{yy} \\ \sigma_{xy} \end{Bmatrix} z^3\, dA + \oint_\Gamma \begin{Bmatrix} \sigma^s_{xx} \\ \sigma^s_{yy} \\ 0 \end{Bmatrix} z^3\, dS \tag{25}$$

$$\begin{Bmatrix} Q_{xz} \\ Q_{yz} \\ R_{xz} \\ R_{yz} \end{Bmatrix} = \int_A \begin{Bmatrix} \sigma_{xz} \\ \sigma_{yz} \\ \sigma_{xz} z^2 \\ \sigma_{yz} z^2 \end{Bmatrix} dA + \oint_\Gamma \begin{Bmatrix} \sigma^s_{xz} \\ \sigma^s_{yz} \\ \sigma^s_{xz} z^2 \\ \sigma^s_{yz} z^2 \end{Bmatrix} dS \tag{26}$$

where $\sigma^k_{xx} = \sigma_{xx} + \frac{\nu}{(1-\nu)}\sigma_{zz}$ and $\sigma^k_{yy} = \sigma_{yy} + \frac{\nu}{(1-\nu)}\sigma_{zz}$

After substituting the values of stresses from Equations (10), and (16)–(22) into Equations (23)–(26), we obtain stress resultants in terms of strains as,

$$\begin{aligned} \begin{Bmatrix} N_{xx} \\ N_{yy} \\ N_{xy} \end{Bmatrix} = & \begin{bmatrix} A_{11} & A_{12} & A_{16} \\ A_{12} & A_{22} & A_{26} \\ A_{16} & A_{26} & A_{66} \end{bmatrix} \begin{Bmatrix} \varepsilon^{(0)}_{xx} \\ \varepsilon^{(0)}_{yy} \\ \gamma^{(0)}_{xy} \end{Bmatrix} + \begin{bmatrix} B_{11} & B_{12} & B_{16} \\ B_{12} & B_{22} & B_{26} \\ B_{16} & B_{26} & B_{66} \end{bmatrix} \begin{Bmatrix} \varepsilon^{(1)}_{xx} \\ \varepsilon^{(1)}_{yy} \\ \gamma^{(1)}_{xy} \end{Bmatrix} \\ & + \begin{bmatrix} E_{11} & E_{12} & E_{16} \\ E_{12} & E_{22} & E_{26} \\ E_{16} & E_{26} & E_{66} \end{bmatrix} \begin{bmatrix} \varepsilon^{(3)}_{xx} \\ \varepsilon^{(3)}_{yy} \\ \gamma^{(3)}_{xy} \end{bmatrix} + (2\mu^s + \lambda^s) \begin{bmatrix} Z_{11} \\ Z_{21} \\ Z_{31} \end{bmatrix} \end{aligned} \tag{27}$$

$$\begin{aligned} \begin{Bmatrix} M_{xx} \\ M_{yy} \\ M_{xy} \end{Bmatrix} = & \begin{bmatrix} B_{11} & B_{12} & B_{16} \\ B_{12} & B_{22} & B_{26} \\ B_{16} & B_{26} & B_{66} \end{bmatrix} \begin{bmatrix} \varepsilon^{(0)}_{xx} \\ \varepsilon^{(0)}_{yy} \\ \gamma^{(0)}_{xy} \end{bmatrix} + \begin{bmatrix} D_{11} & D_{12} & D_{16} \\ D_{12} & D_{22} & D_{26} \\ D_{16} & D_{26} & D_{66} \end{bmatrix} \begin{Bmatrix} \varepsilon^{(1)}_{xx} \\ \varepsilon^{(1)}_{yy} \\ \gamma^{(1)}_{xy} \end{Bmatrix} \\ & + \begin{bmatrix} F_{11} & F_{12} & F_{16} \\ F_{12} & F_{22} & F_{26} \\ F_{16} & F_{26} & F_{66} \end{bmatrix} \begin{Bmatrix} \varepsilon^{(3)}_{xx} \\ \varepsilon^{(3)}_{yy} \\ \gamma^{(3)}_{xy} \end{Bmatrix} + \begin{Bmatrix} L_{11} \\ L_{21} \\ L_{31} \end{Bmatrix} \end{aligned} \tag{28}$$

$$\begin{Bmatrix} P_{xx} \\ P_{yy} \\ P_{xy} \end{Bmatrix} = \begin{bmatrix} E_{11} & E_{12} & E_{16} \\ E_{12} & E_{22} & E_{26} \\ E_{16} & E_{26} & E_{66} \end{bmatrix} \begin{Bmatrix} \varepsilon_{xx}^{(0)} \\ \varepsilon_{yy}^{(0)} \\ \gamma_{xy}^{(0)} \end{Bmatrix} + \begin{bmatrix} F_{11} & F_{12} & F_{16} \\ F_{12} & F_{22} & F_{26} \\ F_{16} & F_{26} & F_{66} \end{bmatrix} \begin{Bmatrix} \varepsilon_{xx}^{(1)} \\ \varepsilon_{yy}^{(1)} \\ \gamma_{xy}^{(1)} \end{Bmatrix} + \begin{bmatrix} H_{11} & H_{12} & H_{16} \\ H_{12} & H_{22} & H_{26} \\ H_{16} & H_{26} & H_{66} \end{bmatrix} \begin{bmatrix} \varepsilon_{xx}^{(3)} \\ \varepsilon_{yy}^{(3)} \\ \gamma_{xy}^{(3)} \end{bmatrix} + \begin{Bmatrix} O_{11} \\ O_{21} \\ O_{31} \end{Bmatrix} \tag{29}$$

$$\begin{Bmatrix} Q_{xz} \\ Q_{yz} \\ R_{xz} \\ R_{yz} \end{Bmatrix} = \begin{Bmatrix} \tau^s \left[\gamma_{xz}^{(0)} (2b+h) + \gamma_{xz}^{(2)} \left(\frac{bh^2}{2} + \frac{h^3}{12} \right) \right] \\ \tau^s \left[\gamma_{yz}^{(0)} (2a+h) + \gamma_{yz}^{(2)} \left(\frac{ah^2}{2} + \frac{h^3}{12} \right) \right] \\ \tau^s \left[\gamma_{xz}^{(0)} \left(\frac{bh^2}{2} + \frac{h^3}{12} \right) + \gamma_{xz}^{(2)} \left(\frac{bh^4}{8} + \frac{h^5}{80} \right) \right] \\ \tau^s \left[\gamma_{yz}^{(0)} \left(\frac{ah^2}{2} + \frac{h^3}{12} \right) + \gamma_{yz}^{(2)} \left(\frac{ah^4}{8} + \frac{h^5}{80} \right) \right] \end{Bmatrix} \tag{30}$$

where Z_{i1}, L_{i1} and O_{i1} $(i = 1, 2, 3)$ are given in the appendix.

$$\{A_{ij}, B_{ij}, D_{ij}, E_{ij}, F_{ij}, H_{ij}\} = \sum_{k=1}^{N} \int_{z_k}^{z_{k+1}} \bar{Q}_{ij}^{(k)} \left(1, z, z^2, z^3, z^4, z^6\right) dz, \quad (i, j = 1, 2, 6) \tag{31}$$

Using Equation (3), the nonlocal stress resultants can be written as

$$\left(1 - \mu\nabla^2\right) \begin{Bmatrix} N_{xx}^{nl} \\ N_{yy}^{nl} \\ N_{xy}^{nl} \end{Bmatrix} = \begin{Bmatrix} N_{xx} \\ N_{yy} \\ N_{xy} \end{Bmatrix} \tag{32}$$

$$\left(1 - \mu\nabla^2\right) \begin{Bmatrix} M_{xx}^{nl} \\ M_{yy}^{nl} \\ M_{xy}^{nl} \end{Bmatrix} = \begin{Bmatrix} M_{xx} \\ M_{yy} \\ M_{xy} \end{Bmatrix} \tag{33}$$

$$\left(1 - \mu\nabla^2\right) \begin{Bmatrix} P_{xx}^{nl} \\ P_{yy}^{nl} \\ P_{xy}^{nl} \end{Bmatrix} = \begin{Bmatrix} P_{xx} \\ P_{yy} \\ P_{xy} \end{Bmatrix} \tag{34}$$

$$\left(1 - \mu\nabla^2\right) \begin{Bmatrix} Q_{xz}^{nl} \\ Q_{yz}^{nl} \\ R_{xz}^{nl} \\ R_{yz}^{nl} \end{Bmatrix} = \begin{Bmatrix} Q_{xz} \\ Q_{yz} \\ R_{xz} \\ R_{yz} \end{Bmatrix} \tag{35}$$

3.5 Equations of equilibrium

The governing equilibrium equations for the Third order shear deformation theory (for laminates) can be derived using the principle of virtual displacement (Hamilton's principle). By substituting the nonlocal stress resultants in terms of displacements into the statement of principle of virtual displacement and integrating by parts, the equations of motion can be obtained as [72]

$$\frac{\partial N_{xx}^{nl}}{\partial x}+\frac{\partial N_{xy}^{nl}}{\partial y}=\left(1-\mu\nabla^2\right)\left(I_0\ddot{u}_0+J_1\ddot{\phi}_x-c_1I_3\frac{\partial\ddot{w}_0}{\partial x}\right) \tag{36}$$

$$\frac{\partial N_{xy}^{nl}}{\partial x}+\frac{\partial N_{yy}^{nl}}{\partial y}=\left(1-\mu\nabla^2\right)\left(I_0\ddot{v}_0+J_1\ddot{\phi}_y-c_1I_3\frac{\partial\ddot{w}_0}{\partial y}\right) \tag{37}$$

$$\begin{aligned}&\frac{\partial\bar{Q}_x^{nl}}{\partial x}+\frac{\partial\bar{Q}_y^{nl}}{\partial y}+\frac{\partial}{\partial x}\left(N_{xx}^{nl}\frac{\partial w_0}{\partial x}+N_{yy}^{nl}\frac{\partial w_0}{\partial y}\right)+\frac{\partial}{\partial y}\left(N_{xy}^{nl}\frac{\partial w_0}{\partial x}+N_{yy}^{nl}\frac{\partial w_0}{\partial y}\right)\\&+c_1\left(\frac{\partial^2P_{xx}^{nl}}{\partial x^2}+2\frac{\partial^2P_{xy}^{nl}}{\partial x\,\partial y}+\frac{\partial^2P_{yy}^{nl}}{\partial y^2}\right)+q=\left(1-\mu\nabla^2\right)\left[I_0\ddot{w}_0-c_1^2I_6\left(\frac{\partial\ddot{w}_0}{\partial x^2}+\frac{\partial^2\ddot{w}_0}{\partial y^2}\right)\right]\\&+\left(1-\mu\nabla^2\right)\left\{c_1\left[I_3\left(\frac{\partial\ddot{u}_0}{\partial x}+\frac{\partial\ddot{v}_0}{\partial y}\right)+J_4\left(\frac{\partial\ddot{\phi}_x}{\partial x}+\frac{\partial\ddot{\phi}_y}{\partial y}\right)\right]\right\}\end{aligned} \tag{38}$$

$$\frac{\partial\bar{M}_{xx}^{nl}}{\partial x}+\frac{\partial\bar{M}_{xy}^{nl}}{\partial y}-\bar{Q}_x^{nl}=\left(1-\mu\nabla^2\right)\left(J_1\ddot{u}_0+K_2\ddot{\phi}_x-c_1J_4\frac{\partial\ddot{w}_0}{\partial x}\right) \tag{39}$$

$$\frac{\partial\bar{M}_{xy}^{nl}}{\partial x}+\frac{\partial\bar{M}_{yy}^{nl}}{\partial y}-\bar{Q}_y^{nl}=\left(1-\mu\nabla^2\right)\left(J_1\ddot{v}_0+K_2\ddot{\phi}_y-c_1J_4\frac{\partial\ddot{w}_0}{\partial y}\right) \tag{40}$$

where

$$\bar{M}_{\alpha\,\beta}^{nl}=M_{\alpha\,\beta}^{nl}-c_1P_{\alpha\,\beta}^{nl}\quad(\alpha,\beta=1,2,6):\quad\bar{Q}_\alpha=Q_\alpha^{nl}-c_2R_\alpha^{nl}\quad(\alpha=4,5) \tag{41}$$

$$I_i=\sum_{k=1}^{N}\int_{z_k}^{z_{k+1}}\rho^{(k)}(z)^i\,dz\quad(i=0,1,2,..,6) \tag{42}$$

$$J_i=I_i-c_1I_{i+2},\quad K_2=I_2-2c_1I_4+c_1^2I_6,\quad c_1=\frac{4}{3h^2},\quad c_2=3c_1 \tag{43}$$

4 Navier's solution procedure

In Navier's method, the generalized displacements are expanded in a double trigonometric series in terms of unknown parameters. The choice of the functions in the series is restricted

to those which satisfy the boundary conditions of the problem. Substitution of the displacement expansions into the governing equations should result in a unique, invertible, set of algebraic equations among the parameters of the expansion. Navier's solution can be developed for rectangular laminates with two sets of simply supported boundary conditions (SS-1 and SS-2). In the following subsections, Navier solutions of cross-ply laminates for the SS-1 boundary conditions and anti-symmetric angle-ply laminates for the SS-2 boundary conditions including nonlocal and surface stress effects are presented (see Reddy [2]).

4.1 Boundary conditions and displacement expansions for SS-1

The SS-1 boundary conditions for third-order shear deformation plate theory are

$$\begin{aligned} &u_0(x,0,t)=0, \quad u_0(x,b,t)=0, \quad v_0(0,y,t)=0, \quad v_0(a,y,t)=0\\ &\phi_x(x,0,t)=0, \quad \phi_x(x,b,t)=0, \quad \phi_y(0,y,t)=0, \quad \phi_y(a,y,t)=0\\ &w_0(x,0,t)=0, \quad w_0(x,b,t)=0, \quad w_0(0,y,t)=0, \quad w_0(a,y,t)=0 \end{aligned} \tag{44}$$

$$\begin{aligned} &N_{xx}(0,y,t)=0, \quad N_{xx}(a,y,t)=0, \quad N_{yy}(x,0,t)=0, \quad N_{yy}(x,b,t)=0\\ &\bar{M}_{xx}(0,y,t)=0, \quad \bar{M}_{xx}(a,y,t)=0, \quad \bar{M}_{yy}(x,0,t)=0, \quad \bar{M}_{yy}(x,b,t)=0 \end{aligned} \tag{45}$$

The following displacement expansions that satisfy SS-1 boundary conditions are used:

$$\begin{aligned} u_0(x,y,t) &= \sum_{n=1}^{\infty}\sum_{m=1}^{\infty} U_{mn}(t)\cos\alpha x\sin\beta y\\ v_0(x,y,t) &= \sum_{n=1}^{\infty}\sum_{m=1}^{\infty} V_{mn}(t)\sin\alpha x\cos\beta y\\ w_0(x,y,t) &= \sum_{n=1}^{\infty}\sum_{m=1}^{\infty} W_{mn}(t)\sin\alpha x\sin\beta y\\ \phi_x(x,y,t) &= \sum_{n=1}^{\infty}\sum_{m=1}^{\infty} X_{mn}(t)\cos\alpha x\sin\beta y\\ \phi_y(x,y,t) &= \sum_{n=1}^{\infty}\sum_{m=1}^{\infty} Y_{mn}(t)\sin\alpha x\cos\beta y \end{aligned} \tag{46}$$

where $\alpha = \frac{m\pi}{a}$ and $\beta = \frac{n\pi}{b}$. U_{mn}, V_{mn}, W_{mn}, X_{mn} and Y_{mn} are coefficients that are to be determined.

4.2 Boundary conditions and displacement expansions for SS-2

The SS-2 boundary conditions for the third-order shear deformation plate theory are

$$\begin{aligned} &u_0(0,y,t)=0, \quad u_0(a,y,t)=0, \quad v_0(x,0,t)=0, \quad v_0(x,b,t)=0 \\ &\phi_x(x,0,t)=0, \quad \phi_x(x,b,t)=0, \quad \phi_y(0,y,t)=0, \quad \phi_y(a,y,t)=0 \\ &w_0(x,0,t)=0, \quad w_0(x,b,t)=0, \quad w_0(0,y,t)=0, \quad w_0(a,y,t)=0 \end{aligned} \tag{47}$$

$$\begin{aligned} &N_{xy}(0,y,t)=0, \quad N_{xy}(a,y,t)=0, \quad N_{xy}(x,0,t)=0, \quad N_{xy}(x,b,t)=0 \\ &\bar{M}_{xx}(0,y,t)=0, \quad \bar{M}_{xx}(a,y,t)=0, \quad \bar{M}_{yy}(x,0,t)=0, \quad \bar{M}_{yy}(x,b,t)=0 \end{aligned} \tag{48}$$

The following displacement expansions that satisfy SS-2 boundary conditions are used:

$$\begin{aligned} u_0(x,y,t) &= \sum_{n=1}^{\infty}\sum_{m=1}^{\infty} U_{mn}(t)\sin\alpha x\cos\beta y \\ v_0(x,y,t) &= \sum_{n=1}^{\infty}\sum_{m=1}^{\infty} V_{mn}(t)\cos\alpha x\sin\beta y \\ w_0(x,y,t) &= \sum_{n=1}^{\infty}\sum_{m=1}^{\infty} W_{mn}(t)\sin\alpha x\sin\beta y \\ \phi_x(x,y,t) &= \sum_{n=1}^{\infty}\sum_{m=1}^{\infty} X_{mn}(t)\cos\alpha x\sin\beta y \\ \phi_y(x,y,t) &= \sum_{n=1}^{\infty}\sum_{m=1}^{\infty} Y_{mn}(t)\sin\alpha x\cos\beta y \end{aligned} \tag{49}$$

4.3 The Navier solutions

For both SS-1 and SS-2, the transverse load $q_z(x,y,t)$ is expressed in double Fourier sine series as

$$\begin{aligned} q_z(x,y,t) &= \sum_{n=1}^{\infty}\sum_{m=1}^{\infty} Q_{mn}(t)\sin\alpha x\sin\beta y \\ Q_{mn}(t) &= \frac{4}{ab}\int_0^a\int_0^b q_z(x,y,t)\sin\alpha x\sin\beta y\,dx\,dy \end{aligned} \tag{50}$$

Substituting the displacement expansions in Equation (**??**) into the governing equations of equilibrium yields the following ordinary differential equations in time:

$$\mathbf{S}\,\boldsymbol{\Delta} + \mathbf{M}\ddot{\boldsymbol{\Delta}} = \mathbf{F} \tag{51}$$

where $\boldsymbol{\Delta}$ is the displacement vector, $\ddot{\boldsymbol{\Delta}}$ is the acceleration vector, $\mathbf{S}$ and $\mathbf{M}$ are the stiffness and mass matrices, respectively. The displacement $\boldsymbol{\Delta}$ and force vector $\mathbf{F}$ are given as

$$\boldsymbol{\Delta} = \begin{Bmatrix} U_{mn} \\ V_{mn} \\ W_{mn} \\ X_{mn} \\ Y_{mn} \end{Bmatrix}, \quad \mathbf{F} = (1 - \mu\nabla^2) \begin{Bmatrix} 0 \\ 0 \\ Q_{mn} \\ 0 \\ 0 \end{Bmatrix}, \quad Q_{mn} = \frac{16q_0}{\pi^2 mn} \text{ for uniform load} \tag{52}$$

The coefficients of the stiffness matrix $\mathbf{S}$ and mass matrix $\mathbf{M}$ for the two types of boundary conditions are given in the subsections to follow.

For static bending analysis we set $\ddot{\boldsymbol{\Delta}}$ to zero and obtain

$$\mathbf{S}\,\boldsymbol{\Delta} = \mathbf{F} \tag{53}$$

For the natural vibration, we assume that the solution is periodic $\boldsymbol{\Delta}(t) = \boldsymbol{\Delta}_0 e^{i\omega t}$, where ω is the frequency of natural vibration and $i = \sqrt{-1}$. Thus, the free vibration problem consists of solving the eigenvalue problem

$$\left(\mathbf{S} - \omega^2\mathbf{M}\right)\boldsymbol{\Delta} = \mathbf{0} \tag{54}$$

4.3.1 Anti-symmetric cross-ply laminate

The coefficients of the stiffness matrix S_{ij} for anti-symmetric cross-ply laminate are

$$\begin{aligned}
S_{11} &= A_{11}\alpha^2 + A_{66}\beta^2 + (2\mu^s + \lambda^s)\left(\alpha^2 h + 2\alpha^2 b\right) \\
S_{12} &= (A_{12} + A_{66})\alpha\beta \\
S_{13} &= -c_1[E_{11}\alpha^2 + (E_{12} + 2E_{66})\beta^2]\alpha - c_1(2\mu^s + \lambda^s)\left(\frac{h^4}{32}\alpha^3 + \frac{bh^3}{4}\alpha^3\right) \\
S_{14} &= \hat{B}_{11}\alpha^2 + \hat{B}_{33}\beta^2 + (2\mu^s + \lambda^s)\left(\frac{-c_1 h^4}{32}\alpha^2 + bh\alpha^2 - \frac{c_1 bh^3}{4}\alpha^2\right) \\
S_{15} &= (\hat{B}_{12} + \hat{B}_{66})\alpha\beta \\
S_{21} &= S_{12} \\
S_{22} &= A_{66}\alpha^2 + A_{22}\beta^2 + (2\mu^s + \lambda^s)\left(\beta^2 h + 2\beta^2 a\right) \\
S_{23} &= -c_1[E_{22}\beta^2 + (E_{12} + 2E_{66})\alpha^2]\beta - c_1(2\mu^s + \lambda^s)\left(\frac{h^4}{32}\beta^3 + \frac{ah^3}{4}\beta^3\right) \\
S_{24} &= (\hat{B}_{12} + \hat{B}_{66})\alpha\beta
\end{aligned}$$

$$
\begin{aligned}
S_{25} &= \hat{B}_{66}\alpha^2 + \hat{B}_{22}\beta^2 + (2\mu^s + \lambda^s)\left(\frac{-c_1 h^4}{32}\beta^2 + ah\beta^2 - \frac{c_1 a h^3}{4}\beta^2\right) \\
S_{31} &= S_{13} - c_1\frac{bh^3}{8}\alpha^3(4\mu^s + \lambda^s) \\
S_{32} &= S_{23} - c_1\frac{ah^3}{8}\beta^3(4\mu^s + \lambda^s) \\
S_{33} &= \bar{A}_{55}\alpha^2 + \bar{A}_{44}\beta^2 + c_1^2[H_{11}\alpha^4 + 2(H_{12} + 2H_{66})\alpha^2\beta^2 + H_{22}\beta^4] \\
&\quad + \frac{c_1\nu h^4\tau^s}{40(1-\nu)}(\alpha^4 + \beta^4 + \alpha^2\beta^2) + (2\mu^s + \lambda^s)\left[\frac{h^7}{448}(c_1^2\alpha^4 + c_1^2\beta^4) + \frac{h^6}{32}(bc_1^2\alpha^4 + ac_1^2\beta^4)\right] \\
S_{34} &= \hat{A}_{55}\alpha - c_1[\hat{F}_{11}\alpha^3 + (\hat{F}_{12} + 2\hat{F}_{66})\alpha\beta^2] \\
&\quad + (2\mu^s + \lambda^s)\left(\frac{-c_1 h^5}{80}\alpha^3 + \frac{c_1^2 h^7}{448}\alpha^3 - \frac{c_1 h^4}{8}b\alpha^3 + \frac{c_1^2 h^6}{32}b\alpha^3\right) \\
S_{35} &= \bar{A}_{44}\beta - c_1[\hat{F}_{22}\beta^3 + (\hat{F}_{12} + 2\hat{F}_{66})\alpha^2\beta] \\
&\quad + (2\mu^s + \lambda^s)\left(\frac{-c_1 h^5}{80}\beta^3 + \frac{c_1^2 h^7}{448}\beta^3 - \frac{c_1 h^4}{8}a\beta^3 + \frac{c_1^2 h^6}{32}a\beta^3\right) \\
S_{41} &= S_{14} + (2\mu^s + \lambda^s)\left(bh\alpha^2 - c_1\frac{bh^3}{8}\alpha^2\right) \\
S_{42} &= S_{24} \\
S_{43} &= S_{34} + \left(\frac{\nu h^2\tau^s}{6(1-\nu)} - \frac{c_1 h^4\nu\tau^s}{40(1-\nu)}\right)(\alpha^3 + \alpha\beta^2) \\
&\quad + (2\mu^s + \lambda^s)\left(\frac{-c_1 h^5}{80}\alpha^3 + \frac{c_1^2 h^7}{448}\alpha^3 - \frac{c_1 h^4}{8}b\alpha^3 + \frac{c_1^2 h^6}{32}b\alpha^3\right) \\
S_{44} &= \bar{A}_{55} + \bar{D}_{11}\alpha^2 + \bar{D}_{66}\beta^2 \\
&\quad + (2\mu^s + \lambda^s)\left(\frac{h^3}{12}\alpha^2 - \frac{c_1 h^5}{40}\alpha^2 - \frac{c_1 bh^4}{4}\alpha^2 + \frac{c_1^2 h^7}{448}\alpha^2 + \frac{c_1^2 bh^6}{32}\alpha^2\right) \\
S_{45} &= (\bar{D}_{12} + \bar{D}_{66})\alpha\beta \\
S_{51} &= S_{15} \\
S_{52} &= S_{25} + (2\mu^s + \lambda^s)\left(ah\beta^2 - c_1\frac{ah^3}{8}\beta^2\right) \\
S_{53} &= S_{35} + \left(\frac{\nu h^2\tau^s}{6(1-\nu)} - \frac{c_1 h^4\nu\tau^s}{40(1-\nu)}\right)(\beta^3 + \beta\alpha^2) \\
&\quad + (2\mu^s + \lambda^s)\left(\frac{-c_1 h^5}{80}\beta^3 + \frac{c_1^2 h^7}{448}\beta^3 - \frac{c_1 h^4}{8}a\beta^3 + \frac{c_1^2 h^6}{32}a\beta^3\right) \\
S_{54} &= S_{45} \\
S_{55} &= \bar{A}_{44} + \bar{D}_{33}\alpha^2 + \bar{D}_{22}\beta^2 + (2\mu^s + \lambda^s\left(\frac{h^3}{12}\beta^2 - \frac{c_1 h^5}{40}\beta^2 - \frac{c_1 ah^4}{4}\alpha^2 + \frac{c_1^2 h^7}{448}\beta^2 + \frac{c_1^2 bh^6}{32}\beta^2\right)
\end{aligned}
\tag{55}
$$

where

$$\begin{aligned}
&\hat{A}_{ij} = A_{ij} - c_1 D_{ij}, \quad \hat{B}_{ij} = B_{ij} - c_1 E_{ij}, \quad \hat{D}_{ij} = D_{ij} - c_1 F_{ij} \qquad (i,j = 1,2,6) \\
&\hat{F}_{ij} = F_{ij} - c_1 H_{ij}, \quad \bar{A}_{ij} = \hat{A}_{ij} - c_1 \hat{D}_{ij} = A_{ij} - 2c_1 D_{ij} + c_1^2 F_{ij} \qquad (i,j = 1,2,6) \\
&\bar{D}_{ij} = \hat{D}_{ij} - c_1 \hat{F}_{ij} = D_{ij} - 2c_1 F_{ij} + c_1^2 H_{ij} \qquad (i,j = 1,2,6)
\end{aligned} \tag{56}$$

The coefficients of the mass matrix M_{ij} are

$$\begin{aligned}
&M_{11} = I_0, \quad M_{22} = I_0 \\
&M_{33} = I_0 + c_1^2 I_6(\alpha^2 + \beta^2) + 2a\rho^s \frac{c_1 h^4 \nu \rho^s}{160(1-\nu)}(\alpha^2 + \beta^2), \quad M_{34} = -c_1 J_4 \alpha \\
&M_{35} = -c_1 J_4 \beta, M_{43} = -\frac{\nu h^2 \rho^s}{6(1-\nu)}\alpha + \frac{c_1 h^4 \nu \rho^s}{160(1-\nu)}\beta \\
&M_{44} = K_2, \quad M_{53} = -\frac{\nu h^2 \rho^s}{6(1-\nu)}\beta + \frac{c_1 h^4 \nu \rho^s}{160(1-\nu)}\alpha \\
&M_{55} = K_2
\end{aligned} \tag{57}$$

where ρ^s is the surface density.

The in-plane stresses in each laminate layer can be computed using Equation (10), where the strains are given as

$$\begin{Bmatrix} \varepsilon_{xx} \\ \varepsilon_{yy} \\ \varepsilon_{xy} \end{Bmatrix} = \sum_{m=1}^{\infty}\sum_{n=1}^{\infty} \begin{Bmatrix} \left(\bar{R}^{xx}_{mn}(1,1) + z\bar{S}^{xx}_{mn}(1,1) + c_1 z^3 \bar{T}^{xx}_{mn}(1,1)\right)\sin\alpha x \sin\beta y \\ \left(\bar{R}^{xx}_{mn}(2,1) + z\bar{S}^{xx}_{mn}(2,1) + c_1 z^3 \bar{T}^{xx}_{mn}(2,1)\right)\sin\alpha x \sin\beta y \\ \left(\bar{R}^{xx}_{mn}(3,1) + z\bar{S}^{xx}_{mn}(3,1) + c_1 z^3 \bar{T}^{xx}_{mn}(3,1)\right)\sin\alpha x \sin\beta y \end{Bmatrix} \tag{58}$$

where

$$\begin{Bmatrix} \bar{R}^{xx}_{mn} \\ \bar{R}^{yy}_{mn} \\ \bar{R}^{xy}_{mn} \end{Bmatrix} = \begin{Bmatrix} -\alpha U_{mn} \\ -\beta V_{mn} \\ \beta U_{mn} + \alpha V_{mn} \end{Bmatrix}, \quad \begin{Bmatrix} \bar{S}^{xx}_{mn} \\ \bar{S}^{yy}_{mn} \\ \bar{S}^{xy}_{mn} \end{Bmatrix} = \begin{Bmatrix} -\alpha X_{mn} \\ -\beta Y_{mn} \\ \beta X_{mn} + \alpha Y_{mn} \end{Bmatrix} \tag{59}$$

$$\begin{Bmatrix} \bar{T}^{xx}_{mn} \\ \bar{T}^{yy}_{mn} \\ \bar{T}^{xy}_{mn} \end{Bmatrix} = \begin{Bmatrix} \alpha X_{mn} + \alpha^2 W_{mn} \\ \beta Y_{mn} + \beta^2 W_{mn} \\ -(\beta X_{mn} + \alpha Y_{mn} + 2\alpha\beta W_{mn}) \end{Bmatrix} \tag{60}$$

The transverse stresses are determined from the following equations

$$\begin{Bmatrix} \sigma_{yz} \\ \sigma_{xz} \end{Bmatrix} = (1 - c_2 z^2) \sum_{m=1}^{\infty}\sum_{n=1}^{\infty} \begin{bmatrix} Q_{44} & 0 \\ 0 & Q_{55} \end{bmatrix} \begin{Bmatrix} (Y_{mn} + \beta W_{mn})\sin\alpha x \cos\beta y \\ (X_{mn} + \alpha W_{mn})\cos\alpha x \sin\beta y \end{Bmatrix} \tag{61}$$

4.3.2 Anti-symmetric angle-ply laminate

The stiffness coefficients S_{ij} for the SS-2 case are given by

$$
\begin{aligned}
S_{11} &= A_{11}\alpha^2 + A_{66}\beta^2 + (2\mu^s + \lambda^s)\left(\alpha^2 h + 2\alpha^2 b\right)\\
S_{12} &= (A_{12} + A_{66})\alpha\beta\\
S_{13} &= -c_1(3E_{16}\alpha^2 + E_{26}\beta^2)\beta - c_1(2\mu^s + \lambda^s)\left(\frac{h^4}{32}\alpha^3 + \frac{bh^3}{4}\alpha^3\right)\\
S_{14} &= 2\hat{B}_{16}\alpha\beta + (2\mu^s + \lambda^s)\left(\frac{-c_1 h^4}{32}\alpha^2 + bh\alpha^2 - \frac{c_1 bh^3}{4}\alpha^2\right)\\
S_{15} &= \hat{B}_{16}\alpha^2 + \hat{B}_{26}\beta^2, \qquad S_{21} = S_{12}\\
S_{22} &= A_{66}\alpha^2 + A_{22}\beta^2 + (2\mu^s + \lambda^s)\left(\beta^2 h + 2\beta^2 a\right)\\
S_{23} &= -c_1(E_{16}\alpha^2 + 3E_{26}\beta^2)\alpha - c_1(2\mu^s + \lambda^s)\left(\frac{h^4}{32}\beta^3 + \frac{ah^3}{4}\beta^3\right)\\
S_{24} &= S_{15}\\
S_{25} &= 2\hat{B}_{26}\alpha\beta + (2\mu^s + \lambda^s)\left(\frac{-c_1 h^4}{32}\beta^2 + ah\beta^2 - \frac{c_1 ah^3}{4}\beta^2\right)\\
S_{31} &= S_{13} + c_1\frac{bh^3}{8}\alpha^3(4\mu^s + \lambda^s)\\
S_{32} &= S_{23} + c_1\frac{ah^3}{8}\beta^3(4\mu^s + \lambda^s)\\
S_{33} &= \bar{A}_{55}\alpha^2 + \bar{A}_{44}\beta^2 + c_1^2[H_{11}\alpha^4 + 2(H_{12} + 2H_{66})\alpha^2\beta^2 + H_{22}\beta^4]\\
&\quad + \frac{c_1\nu h^4\tau^s}{40(1-\nu)}(\alpha^4 + \beta^4 + \alpha^2\beta^2) + (2\mu^s + \lambda^s)\left[\frac{h^7}{448}(c_1^2\alpha^4 + c_1^2\beta^4) + \frac{h^6}{32}(bc_1^2\alpha^4 + ac_1^2\beta^4)\right]
\end{aligned}
\tag{62}
$$

$$
\begin{aligned}
S_{34} &= \hat{A}_{55}\alpha - c_1[\hat{F}_{11}\alpha^3 + (\hat{F}_{12} + 2\hat{F}_{66})\alpha\beta^2]\\
&\quad + (2\mu^s + \lambda^s)\left(\frac{-c_1 h^5}{80}\alpha^3 + \frac{c_1^2 h^7}{448}\alpha^3 - \frac{c_1 h^4}{8}b\alpha^3 + \frac{c_1^2 h^6}{32}b\alpha^3\right)\\
S_{35} &= \bar{A}_{44}\alpha - c_1[\hat{F}_{22}\beta^3 + (\hat{F}_{12} + 2\hat{F}_{66})\alpha^2\beta^2]\\
&\quad + (2\mu^s + \lambda^s)\left(\frac{-c_1 h^5}{80}\beta^3 + \frac{c_1^2 h^7}{448}\beta^3 - \frac{c_1 h^4}{8}a\beta^3 + \frac{c_1^2 h^6}{32}a\beta^3\right)\\
S_{41} &= S_{14} + (2\mu^s + \lambda^s)\left(bh\alpha^2 - c_1\frac{bh^3}{8}\alpha^2\right)
\end{aligned}
$$

$$
\begin{aligned}
S_{42} &= S_{24} \\
S_{43} &= S_{34} + \left(\frac{\nu h^2 \tau^s}{6(1-\nu)} - \frac{c_1 h^4 \nu \tau^s}{40(1-\nu)}\right)(\alpha^3 + \alpha\beta^2) \\
S_{44} &= \bar{A}_{55} + \bar{D}_{11}\alpha^2 + \bar{D}_{66}\beta^2 \\
&\quad + (2\mu^s + \lambda^s)\left(\frac{h^3}{12}\alpha^2 - \frac{c_1 h^5}{40}\alpha^2 - \frac{c_1 b h^4}{4}\alpha^2 + \frac{c_1^2 h^7}{448}\alpha^2 + \frac{c_1^2 b h^6}{32}\alpha^2\right) \\
S_{45} &= (\bar{D}_{12} + \bar{D}_{66})\alpha\beta, \qquad S_{51} = S_{15} \\
S_{52} &= S_{25} + (2\mu^s + \lambda^s)\left(ah\beta^2 - c_1\frac{ah^3}{8}\beta^2\right) \\
S_{53} &= S_{35} + \left(\frac{\nu h^2 \tau^s}{6(1-\nu)} - \frac{c_1 h^4 \nu \tau^s}{40(1-\nu)}\right)(\beta^3 + \beta\alpha^2) \\
&\quad + (2\mu^s + \lambda^s)\left(\frac{-c_1 h^5}{80}\beta^3 + \frac{c_1^2 h^7}{448}\beta^3 - \frac{c_1 h^4}{8}a\beta^3 + \frac{c_1^2 h^6}{32}a\beta^3\right) \\
S_{54} &= S_{45} \\
S_{55} &= \bar{A}_{44} + \bar{D}_{33}\alpha^2 + \bar{D}_{22}\beta^2 + (2\mu^s + \lambda^s)\left(\frac{h^3}{12}\beta^2 - \frac{c_1 h^5}{40}\beta^2 - \frac{c_1 a h^4}{4}\alpha^2 + \frac{c_1^2 h^7}{448}\beta^2 + \frac{c_1^2 b h^6}{32}\beta^2\right)
\end{aligned}
$$

The coefficients of the mass matrix for anti-symmetric angle-ply laminates are same as those in Equation (57). The in-plane stresses in each laminate layer can be computed using the equation (10) where the strains are given as

$$
\begin{Bmatrix} \varepsilon_{xx}^{(0)} \\ \varepsilon_{yy}^{(0)} \\ \varepsilon_{xy}^{(0)} \end{Bmatrix} = \sum_{m=1}^{\infty}\sum_{n=1}^{\infty} \begin{Bmatrix} \alpha U_{mn} \cos\alpha x \cos\beta y \\ \beta V_{mn} \cos\alpha x \cos\beta y \\ -(\beta U_{mn} + \alpha V_{mn}) \sin\alpha x \sin\beta y \end{Bmatrix} \tag{63}
$$

$$
\begin{Bmatrix} \varepsilon_{xx}^{(1)} \\ \varepsilon_{yy}^{(1)} \\ \varepsilon_{xy}^{(1)} \end{Bmatrix} = -\sum_{m=1}^{\infty}\sum_{n=1}^{\infty} \begin{Bmatrix} \alpha X_{mn} \sin\alpha x \sin\beta y \\ \beta Y_{mn} \cos\alpha x \cos\beta y \\ -(\beta X_{mn} + \alpha Y_{mn}) \cos\alpha x \cos\beta y \end{Bmatrix} \tag{64}
$$

$$
\begin{Bmatrix} \varepsilon_{xx}^{(3)} \\ \varepsilon_{yy}^{(3)} \\ \varepsilon_{xy}^{(3)} \end{Bmatrix} = c_1 \sum_{m=1}^{\infty}\sum_{n=1}^{\infty} \begin{Bmatrix} (\alpha X_{mn} + \alpha^2 W_{mn}) \sin\alpha x \sin\beta y \\ (\beta Y_{mn} + \beta_2 W_{mn}) \sin\alpha x \sin\beta y \\ -(\beta X_{mn} + \alpha Y_{mn} + 2\alpha\beta W_{mn}) \cos\alpha x \cos\beta y \end{Bmatrix} \tag{65}
$$

5 Numerical Examples

5.1 Preliminary comments

In this section we present several examples of the analytical solutions obtained in this study. Navier's solution is obtained using 100 terms in the series for uniformly distributed load. Both bending and free vibration solutions are presented for each problem. The following three examples are considered:

(1) Isotropic plates with following material properties $E = 30 \times 10^6$ Mpa, $\nu = 0.3$, $a = 10$ mm, $q_0 = 1$, and $\rho = 1$, and subjected to a uniformly distributed transverse load of intensity q_0.

(2) Antisymmetric cross-ply $(0°/90°/0°/90°)$ laminated plates.

(3) Antisymmetric angle-ply $(30°/-30°/30°/-30°)$ laminated plates.

For all examples the thickness of all layers are equal and each layer is orthotropic with following material properties: $E_1 = 175\times10^3$ MPa, $E_2 = 7\times10^3$ MPa, $G_{12} = 3.5\times10^3$ MPa, $G_{13} = 3.5 \times 10^3$ MPa, $G_{23} = 1.4 \times 10^3$ MPa, $\nu_{12} = 0.25$, $\nu_{13} = 0.25$, $\nu_{21} = (E_2/E_1)\nu_{12}$, and $a = 20$ mm. The following notations are used for deflection and frequency namely: $\bar{w}^{nl}$ is the dimensionless maximum deflection with nonlocal effect; $\bar{w}^{s}$ is the dimensionless maximum deflection with surface effect; $\bar{w}^{nls}$ dimensionless maximum deflection with nonlocal and surface effect. $\bar{\omega}^{nl}$ dimensionless fundamental frequency with nonlocal effect; $\bar{\omega}^{s}$ dimensionless first mode frequency with surface effect. $\bar{\omega}^{nls}$ dimensionless fundamental frequency with nonlocal and surface effect. For the isotropic plate example, the dimensionless maximum center deflection, fundamental frequency, respectively, are obtained as $\bar{w} = w_0 \times (Eh^3/q_0a^4) \times 10^2$, $\bar{\omega} = \omega h\sqrt{\rho/G}$. For all the laminated plate examples, the maximum center deflection, and fundamental frequency are dimensionless as $\bar{w} = w \times (E_2h^3/q_0a^4) \times 10^2$ and $\bar{\omega} = \omega h\sqrt{\rho/G_{13}}$, where a, b, and h are the length, width and thickness of the plate, respectively; q_0 is the intensity of the uniformly distributed transverse load and ρ is the material density; E and G are Young's and shear moduli, respectively. The dimensionless stress measures used are

$$\begin{aligned} \bar{\sigma}_{xx} &= \sigma_{xx}\Big(\frac{a}{2}, \frac{b}{2}, \frac{h}{2}\Big)\Big(\frac{h^2}{b^2q_0}\Big), \quad \bar{\sigma}_{yy} = \sigma_{yy}\Big(\frac{a}{2}, \frac{b}{2}, \frac{h}{2}\Big)\Big(\frac{h^2}{b^2q_0}\Big) \\ \bar{\tau}_{yz} &= \tau_{yz}\Big(\frac{a}{2}, 0, 0\Big)\Big(\frac{h}{bq_0}\Big), \qquad \bar{\tau}_{xz} = \tau_{xz}\Big(0, \frac{b}{2}, 0\Big)\Big(\frac{h}{bq_0}\Big) \end{aligned} \tag{66}$$

Table 1: Comparison of dimensionless maximum deflection, stresses, and fundamental frequency considering nonlocal and surface effects.

a/b	a/h	μ	τ^s (N/m)	$\bar{w}$	$\bar{\omega}$	$\bar{\sigma}_{xx}$	$\bar{\sigma}_{yy}$	$\bar{\tau}_{yz}$	$\bar{\tau}_{xz}$
1	10	0	0.0	3.12158	4.67311	0.28817	0.28817	0.45601	0.45601
		0	1.7	3.12158	4.67311	0.28817	0.28817	0.45600	0.45600
		0	3.4	3.12157	4.67312	0.28816	0.28816	0.45600	0.45600
		0	6.8	3.12157	4.67312	0.28816	0.28816	0.45600	0.45600
		1	0.0	2.33344	5.50767	0.32446	0.32446	0.99054	0.99054
		3	0.0	1.70051	7.17679	0.39105	0.39105	2.05960	2.05960
		5	0.0	1.40336	8.84591	0.45954	0.45954	3.12866	3.12866
		1	1.7	2.33344	5.50765	0.32447	0.32447	0.99054	0.99054
		3	3.4	1.70051	7.17678	0.39108	0.39108	2.05960	2.05960
		5	6.8	1.40335	8.84592	0.45955	0.45955	3.12866	3.12866
1	20	0	0.0	6.02405	4.49614	0.28749	0.288171	0.46252	0.46252
		0	1.7	6.02405	4.49615	0.28749	0.287488	0.45252	0.45252
		0	3.4	6.02405	4.49616	0.28749	0.287489	0.46252	0.46252
		0	6.8	6.02406	4.49617	0.28749	0.28749	0.46252	0.46252
		1	0.0	4.50309	5.30811	0.32345	0.32346	1.00854	1.00854
		3	0.0	3.28214	6.93205	0.39539	0.39539	2.10057	2.10057
		5	0.0	2.70821	8.55599	0.46733	0.46733	3.12606	3.12606
		1	1.7	4.50308	5.30812	0.32346	0.32346	1.00854	1.00854
		3	3.4	3.28214	6.93206	0.39539	0.39539	2.10057	2.10057
		5	6.8	2.70821	8.55600	0.46733	0.46733	3.12605	3.12605

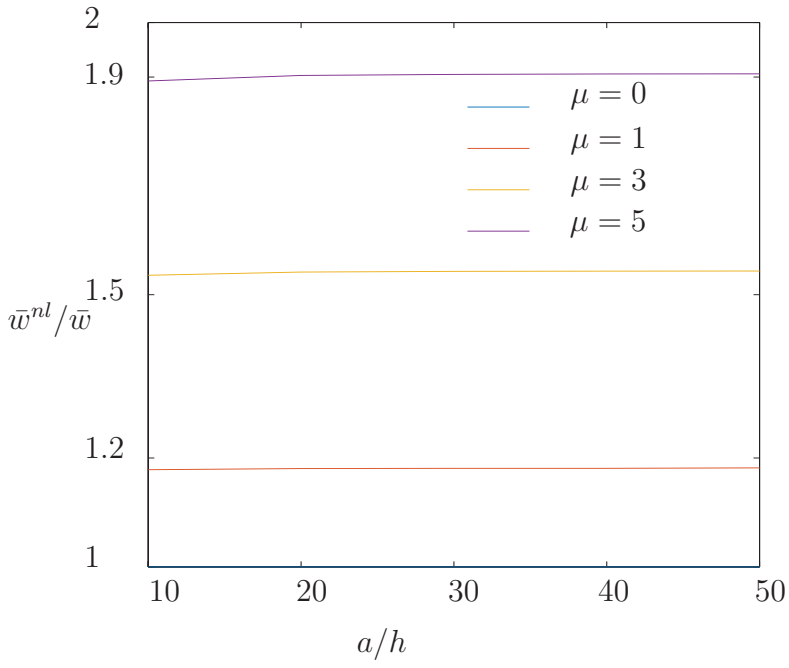

(a)

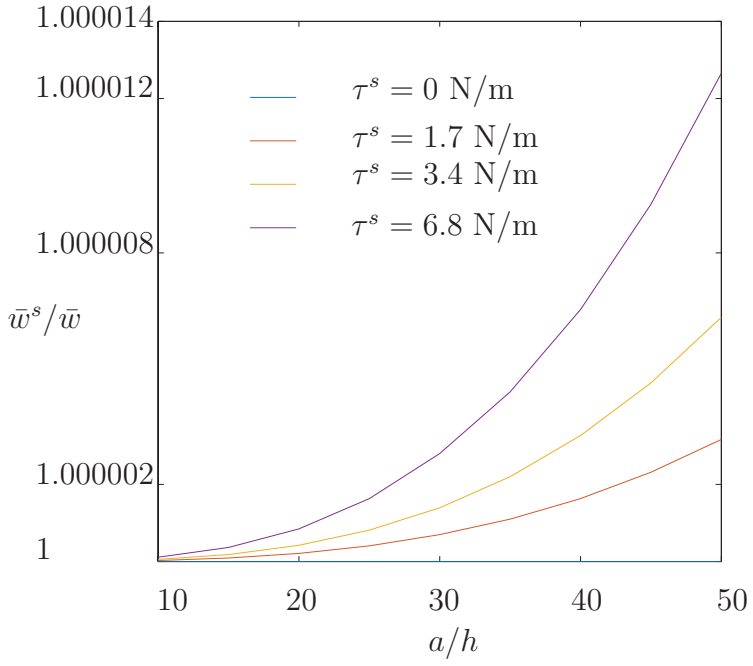

(b)

Figure 1: (a)Deflection ratio $\bar{w}^{nl}/\bar{w}$ versus a/h for various values of μ and $\tau^s = 0$. (b) Deflection ratio versus a/h for various values of τ^s and $\mu = 0$.

5.2 Isotropic plates

A simply supported isotropic square plate subjected to a uniformly distributed transverse load is considered. Both static bending and free vibration analysis has been performed. Table 1 shows the nondimensional maximum values of deflections, stresses and fundamental frequency. Two different aspect ratios of $a/h = 10$ and $a/h = 20$ are considered. The nonlocal parameter μ and surface effect parameter τ^s are varied. It is observed that the maximum values of the dimensionless deflection increases with increase in nonlocal parameters μ and τ^s. The dimensionless frequency decreases with an increase in nonlocal parameters. For a fixed nonlocal parameter an increase in surface parameter has a stiffening effect and there is a decrease in the maximum deflection and increase in the frequency as given in Table 1. The rate of change in the solutions for the surface effect is quite small; the change is not seen in some cases unless additional decimal places are reported.

Figure 1 (a) shows the variation of deflection ratio $\bar{w}^{nl}/\bar{w}$ (ratio of dimensionless maximum deflection with nonlocal effect to the dimensionless maximum deflection with out nonlocal effect) with increasing values of a/h. Figure 1(b) shows variation of deflection ratio $\bar{w}^s/\bar{w}$ with increasing values of a/h where $\bar{w}^s/\bar{w}$ is the ratio of dimensionless maximum deflection with surface effect to the dimensionless maximum deflection with out surface effect. It is observed that the ratio increases as the value of a/h increases.

Figure 2 (a) shows the variation of deflection ratio $\bar{w}^{nls}/\bar{w}$ with increasing values of a/h. Figure 2(b) shows the variation of frequency ratio i.e $\bar{\omega}^{nls}/\bar{\omega}$ with increasing values of a/h where $\bar{\omega}^{nls}/\bar{\omega}$ is the ratio of dimensionless fundamental frequency with nonlocal effect to the dimensionless fundamental frequency without the nonlocal effect.

Figure 3(a) shows the variation of frequency ratio $\bar{\omega}^s/\bar{\omega}$ with increasing values of a/h where $\bar{\omega}^s/\bar{\omega}$ is the ratio of dimensionless fundamental frequency with surface effect to the dimensionless fundamental frequency without the surface effect. Figure 3(b) shows the variation of frequency ratio $\bar{\omega}^{nls}/\bar{\omega}$ with increasing values of a/h where $\bar{\omega}^{nls}/\bar{\omega}$ is the ratio of dimensionless fundamental frequency with surface and nonlocal effect to the dimensionless fundamental frequency with no surface and nonlocal effects. As stated earlier, the rate of change in the solutions for the surface effect is quite small.

Figure 4(a), Figure 4(b), Figure 5(a), Figure 5(b) respectively shows the variation of $\bar{\sigma}_{xx}$, $\bar{\sigma}_{yy}$,$\bar{\tau}_{yz}$,$\bar{\tau}_{xz}$ with thickness coordinate z/h for various values of nonlocal parameter μ. The plot clearly indicates that the nonlocal parameter has a significant effect on the stresses.

5.3 Antisymmetric cross-ply ($0^\circ/90^\circ/0^\circ/90^\circ$) laminated plates

A simply supported square antisymmetric cross ply laminated plate subjected to a uniformly distributed transverse load is considered. Both static bending and free vibration analysis has been performed. Table 2 shows the dimensionless maximum deflections, stresses and

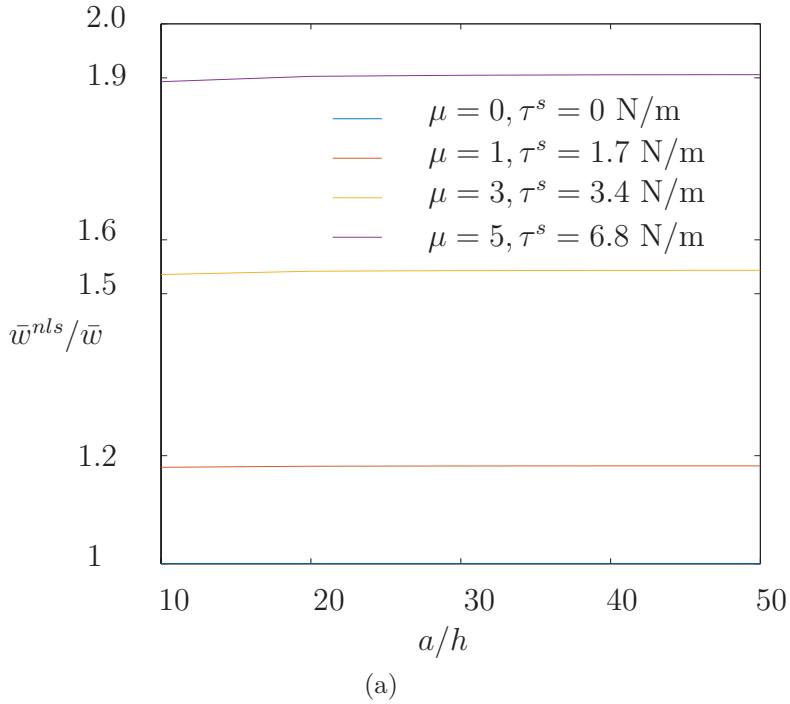

(a)

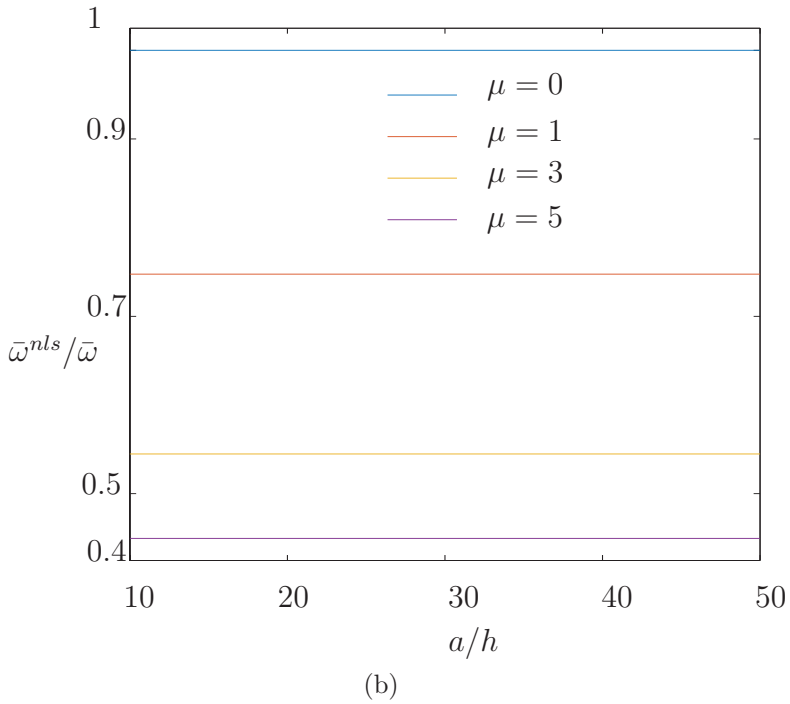

(b)

Figure 2: (a)Deflection ratio versus a/h for various values of μ and τ^s,(b) Frequency ratio versus a/h for various values of μ and $\tau^s = 0$

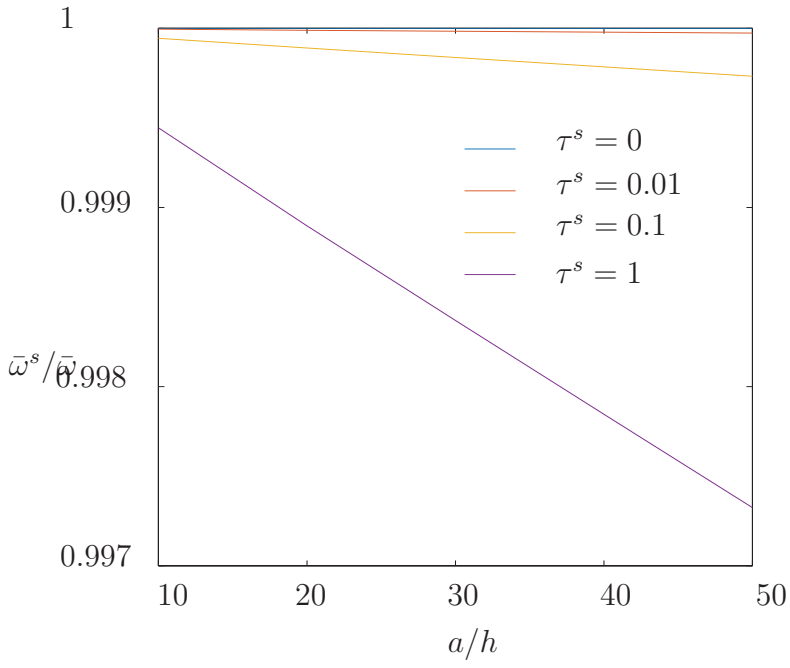

(a)

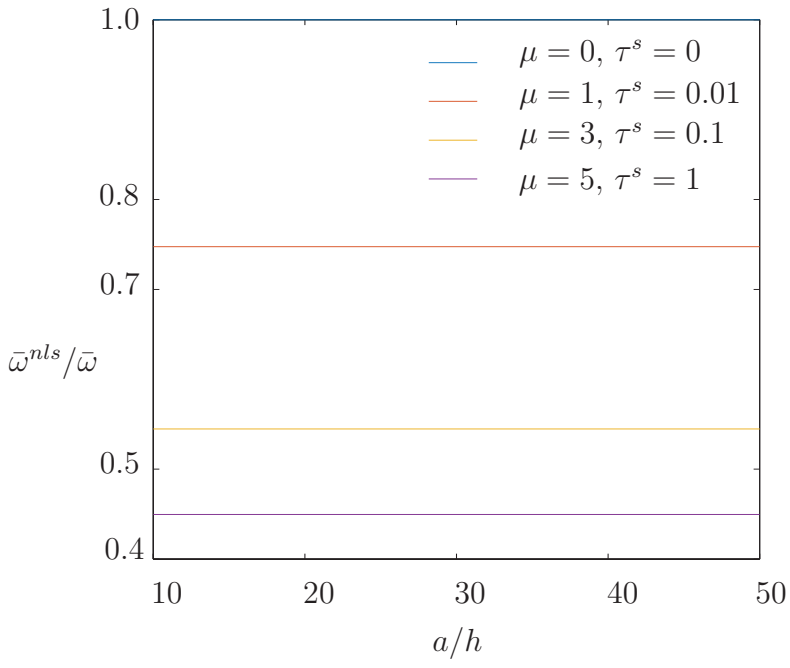

(b)

Figure 3: (a)Frequency ratio versus a/h for various values of τ^s,(b) Frequency ratio versus a/h for various values of μ and τ^s

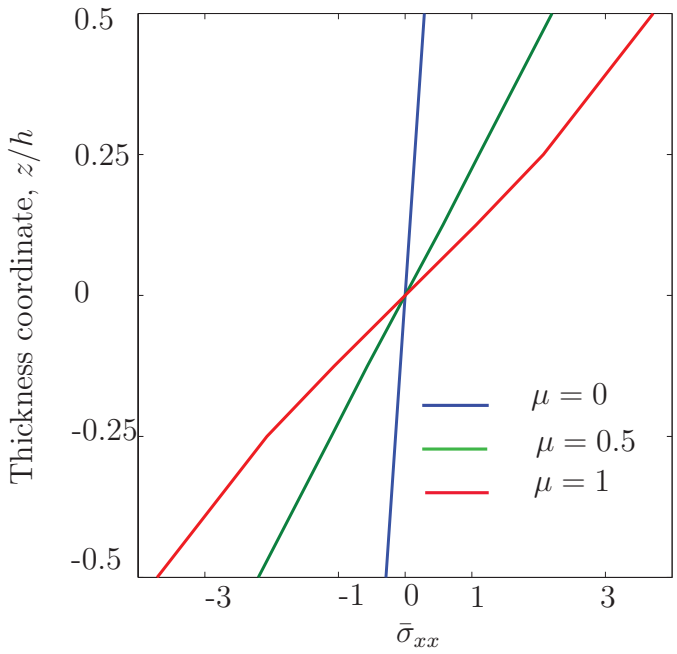

(a)

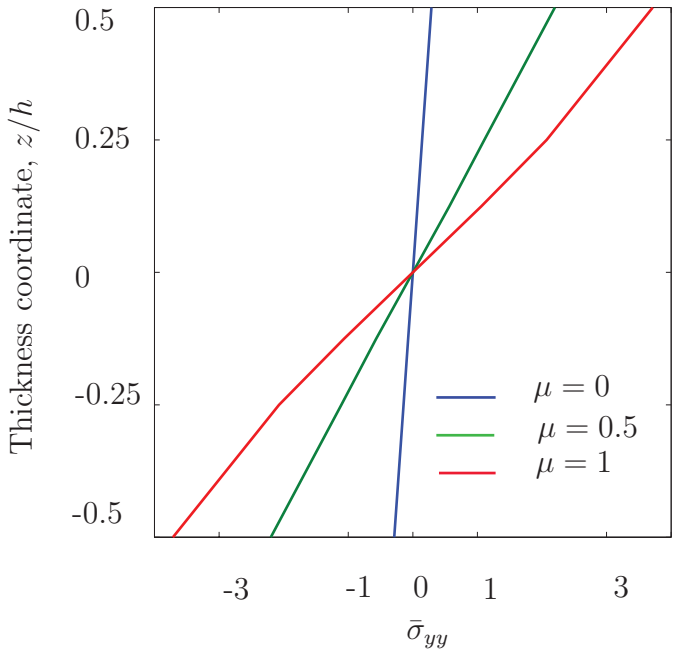

(b)

Figure 4: (a) Distribution of $\bar{\sigma}_{xx}$ predicted by both local and nonlocal TSDT (b) Distribution of $\bar{\sigma}_{yy}$ predicted by both local and nonlocal TSDT

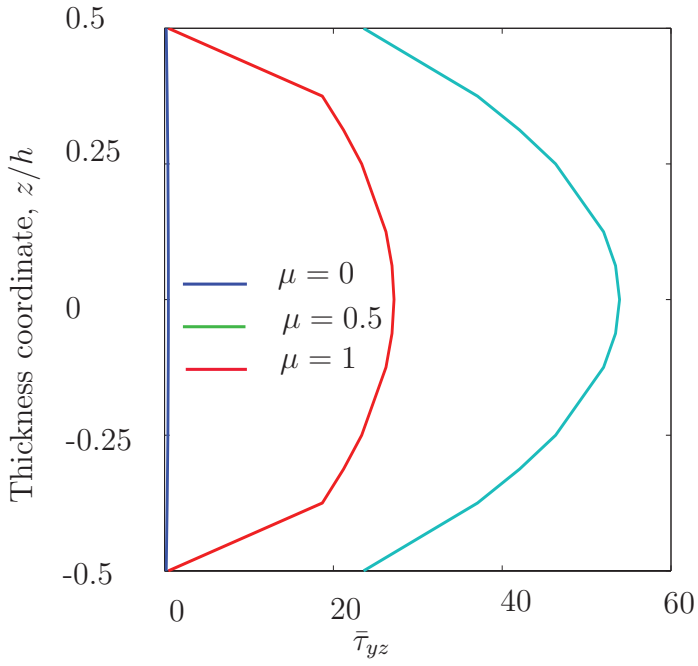

(a)

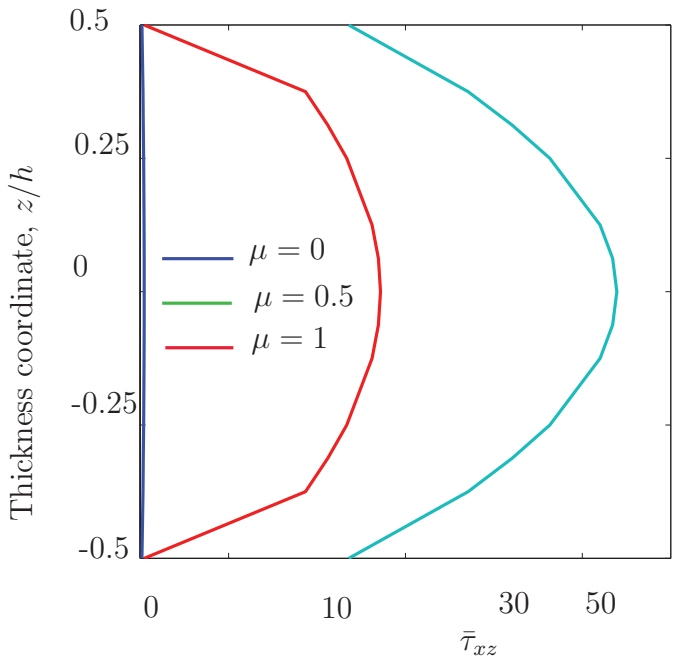

(b)

Figure 5: (a) Distribution of $\bar{\tau}_{yz}$ predicted by both local and nonlocal TSDT (b) Distribution of $\bar{\tau}_{xz}$ predicted by both local and nonlocal TSDT

Table 2: Dimensionless maximum deflections and stresses in simply supported antisymmetric cross-ply laminate (0/90/0/90) under sinusoidally distributed transverse load

a/b	a/h	μ	τ^s (N/m)	$\bar{w}$	$\bar{\omega}$	$\bar{\sigma}_{xx}$	$\bar{\sigma}_{yy}$	$\bar{\tau}_{yz}$	$\bar{\tau}_{xz}$
1	10	0	0.0	1.05268	0.02440	0.74527	0.69058	0.62303	0.62303
		0	1.7	1.05271	0.02440	0.74529	0.69060	0.62303	0.62303
		0	3.4	1.05273	0.02440	0.7453	0.69062	0.62303	0.62302
		0	6.8	1.05276	0.02440	0.74534	0.69066	0.623022	0.62302
		1	0.0	1.05314	0.01824	0.74546	0.69086	0.62471	0.62471
		3	0.0	1.05405	0.01329	0.74585	0.69141	0.62808	0.62808
		5	0.0	1.05496	0.01097	0.74624	0.69196	0.62145	0.62145
		1	1.7	1.05316	0.01824	0.74548	0.69088	0.62470	0.62470
		3	3.4	1.05409	0.01330	0.74589	0.69144	0.62807	0.62808
		5	6.8	1.05504	0.01097	0.74632	0.69203	0.62144	0.62143
	20	0	0.0	0.86949	0.01235	0.73810	0.69693	0.63228	0.63228
		0	1.7	0.86963	0.01235	0.73830	0.69705	0.63227	0.63227
		0	3.4	0.86976	0.01235	0.73840	0.69718	0.63227	0.63226
		0	6.8	0.86003	0.01235	0.73870	0.69742	0.63225	0.63225
		1	0.0	0.86959	0.00923	0.73825	0.69700	0.63273	0.63273
		3	0.0	0.86979	0.00673	0.73837	0.69713	0.63364	0.63364
		5	0.0	0.86999	0.00555	0.73850	0.69727	0.63454	0.63454
		1	1.7	0.86972	0.00923	0.73838	0.69712	0.63273	0.63272
		3	3.4	0.87006	0.00672	0.73863	0.69726	0.63345	0.63362
		5	6.8	0.87053	0.00550	0.73902	0.69776	0.63451	0.63450

first mode frequency for aspect ratio of $a/h = 10$ and $a/h = 20$ with nonlocal and surface effects. The dimensionless stresses are computed as before except $\bar{\sigma}_{yy}$ is now computed at $h/4$. The nonlocal parameter μ and surface effect parameter τ^s are varied. It is observed that the maximum values of the dimensionless deflection increases with increase in nonlocal parameter. The dimensionless frequency decreases with increase in nonlocal parameter. For a fixed nonlocal parameter an increase in surface parameter there is a increase in the maximum deflection and decrease in the frequency as given in Table 2.

Figure 6(a), Figure 6(b), Figure 7(a), Figure 7(b) respectively shows the variation of $\bar{\sigma}_{xx}$, $\bar{\sigma}_{xx}$, $\bar{\tau}_{yz}$, and $\bar{\tau}_{xz}$ with thickness coordinate z/h for various values of nonlocal parameter μ clearly indicating the dependence of stresses on nonlocal parameter.

5.4 Antisymmetric angle-ply $(30^\circ/-30^\circ/30^\circ/-30^\circ)$ plates

An simply supported square antisymmetric angle-ply laminated plate subjected to a uniformly distributed load is considered for static bending and free vibration analysis. Table 3 shows the dimensionless maximum deflections, stresses and first mode frequency for $a/h = 10, 20$ with nonlocal and surface effects. The nonlocal parameter μ and surface effect parameter τ^s are varied. It is observed that the maximum values of the dimensionless deflection increases with increase in nonlocal parameter. The dimensionless frequency decreases with increase in nonlocal parameter. For a fixed nonlocal parameter an increase in surface parameter there is a increase in the maximum deflection and decrease in the frequency as given in Table 3.

Figures 8(a), 8(b), 9(a), and 9(b), respectively, show the variation of $\bar{\sigma}_{xx}$, $\bar{\sigma}_{xx}$, $\bar{\tau}_{yz}$, and $\bar{\tau}_{xz}$ with thickness coordinate z/h for various values of the nonlocal parameter μ.

6 Conclusions

In this work, we have presented analytical solutions for laminated composite plates using the Reddy nonlocal third-order shear deformation theory considering the surface stress effects. The nonlocal theory considers the size effect by assuming that stress at a point depends on the strain at that point as well as on strains at the neighbouring points. Analytical (Navier's) solutions of bending and vibration of a simply supported composite laminated and isotropic plates are developed using this theory to illustrate the effect of nonlocality and surface stress on deflection and vibration frequencies for various span-to-thickness (a/h) ratios. The results indicate that the maximum center deflections increase with an increase in the nonlocal parameter μ and surface stress parameter τ^s, latter having relatively less effect. The opposite is observed for frequencies. The difference in solutions between the two theories decreases as the value of a/h increases. Thus, the parameters associated with the

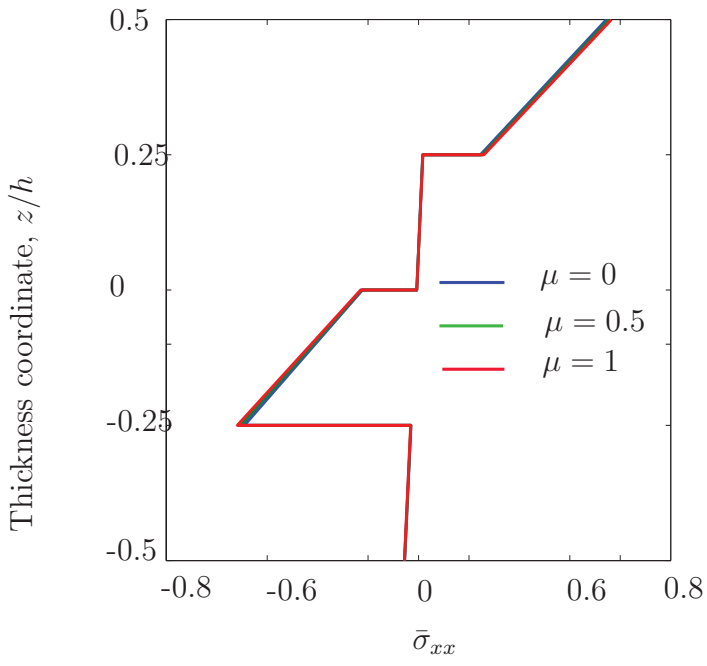

(a)

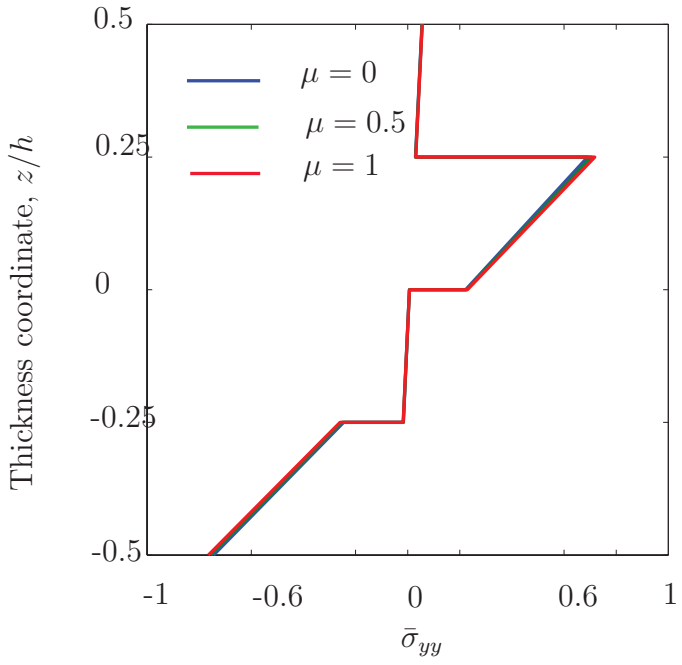

(b)

Figure 6: Distribution of normal stress predicted by both local and nonlocal TSDT for $a/h = 10$ (a) $\bar{\sigma}_{xx}$ (b) $\bar{\sigma}_{yy}$

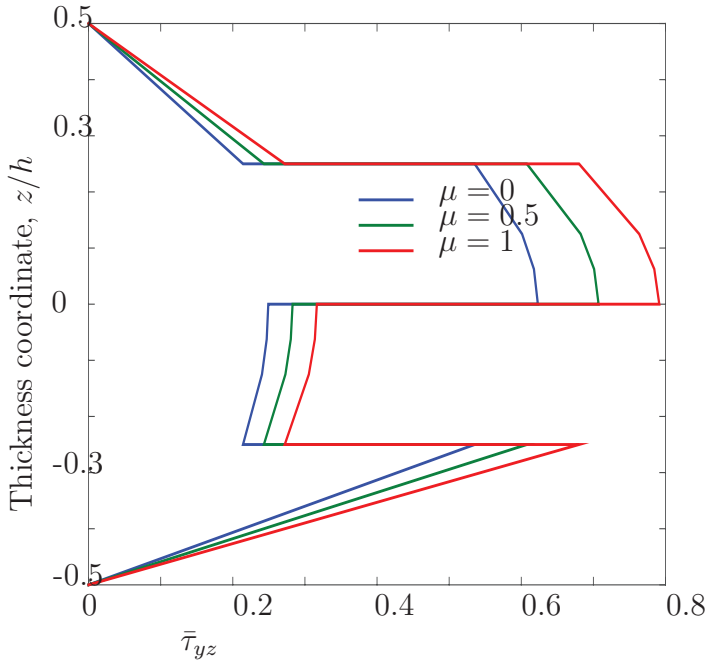

(a)

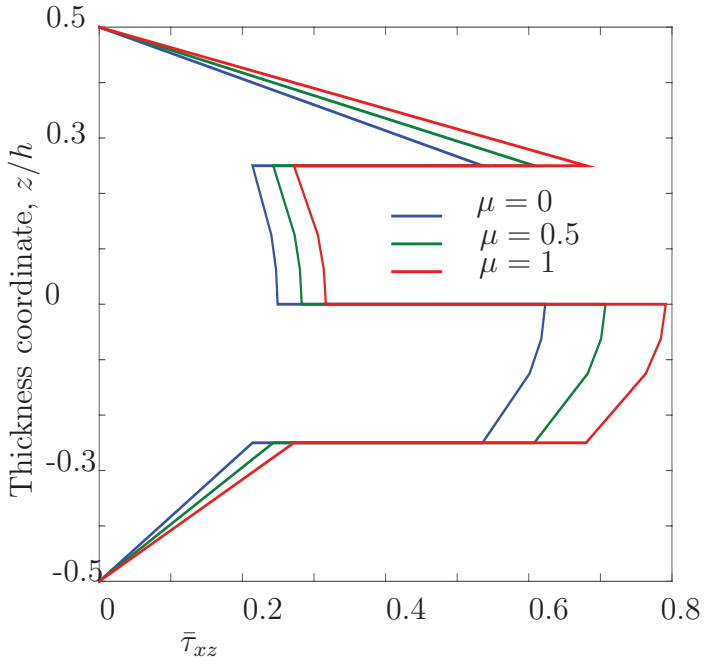

(b)

Figure 7: Distribution of shear stress predicted by both local and nonlocal TSDT for $a/h = 10$ (a) $\bar{\tau}_{yz}$ (b) $\bar{\tau}_{xz}$

Table 3: Dimensionless maximum deflections, fundamental frequencies, and stresses in simply supported (SS-2) antisymmetric angle-ply laminates $(30/-30/30/-30)$ under sinusoidally distributed transverse load

a/b	a/h	μ	τ^s (N/m)	$\bar{w}$	$\bar{\omega}$	$\bar{\sigma}_{xx}$	$\bar{\sigma}_{yy}$	$\bar{\tau}_{yz}$	$\bar{\tau}_{xz}$
1	10	0	0.0	0.74203	0.16985	0.36808	0.14231	0.64644	0.887065
		0	1.7	0.74204	0.16985	0.368085	0.14231	0.64644	0.887064
		0	3.4	0.74205	0.16985	0.36809	0.14231	0.64644	0.887061
		0	6.8	0.74206	0.16985	0.3681	0.14232	0.64644	0.887059
		1	0.0	0.74956	0.12696	0.36951	0.14280	0.75265	1.01536
		3	0.0	0.76463	0.09254	0.37238	0.14379	0.96506	1.27196
		5	0.0	0.77970	0.07635	0.37525	0.14477	1.17746	1.52856
		1	1.7	0.74957	0.12696	0.36952	0.14280	0.75265	1.01535
		3	3.4	0.76465	0.09254	0.37239	0.14379	0.96505	1.27195
		5	6.8	0.77973	0.07636	0.37528	0.14478	1.17745	1.52855
	20	0	0.0	0.55072	0.08552	0.32459	0.12745	0.58790	0.95253
		0	1.7	0.55077	0.08552	0.32463	0.12746	0.58789	0.95253
		0	3.4	0.55083	0.08552	0.32466	0.12748	0.58787	0.95254
		0	6.8	0.55094	0.08552	0.32473	0.12750	0.58784	0.95254
		1	0.0	0.55213	0.06393	0.32471	0.12752	0.61420	0.98801
		3	0.0	0.55494	0.04659	0.32496	0.12768	0.66679	1.05897
		5	0.0	0.55775	0.03845	0.32521	0.12783	0.71938	1.12993
		1	1.7	0.55218	0.06393	0.32475	0.12754	0.61419	0.98802
		3	3.4	0.55505	0.04659	0.32503	0.12771	0.66676	1.05898
		5	6.8	0.55796	0.03845	0.32535	0.12789	0.71931	1.12995

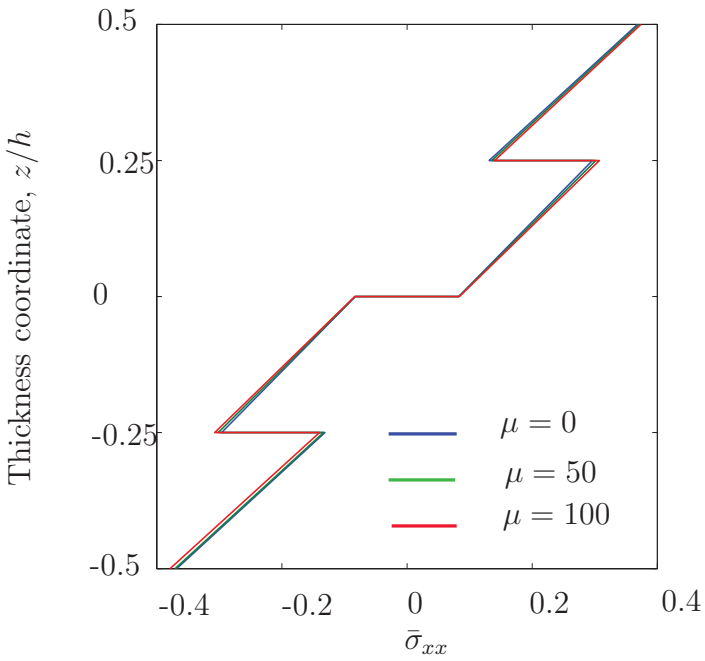

(a)

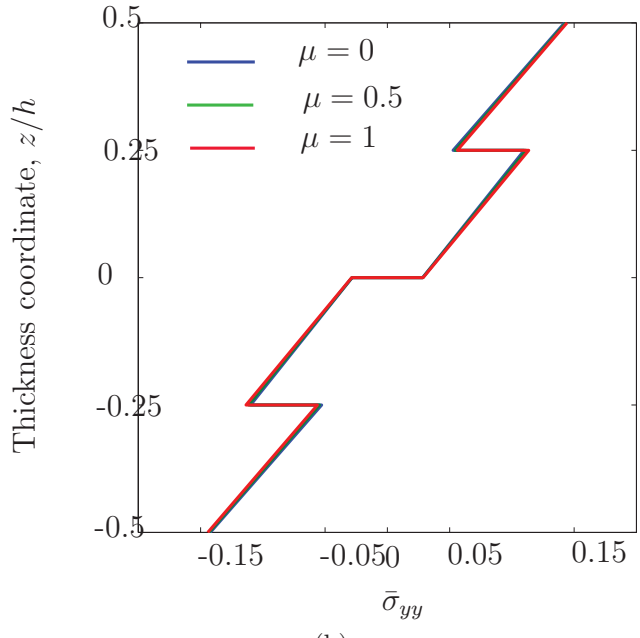

(b)

Figure 8: Distribution of normal stresses predicted by both local and nonlocal TSDT for $a/h = 10$ (a) $\bar{\sigma}_{xx}$ (b) $\bar{\sigma}_{yy}$

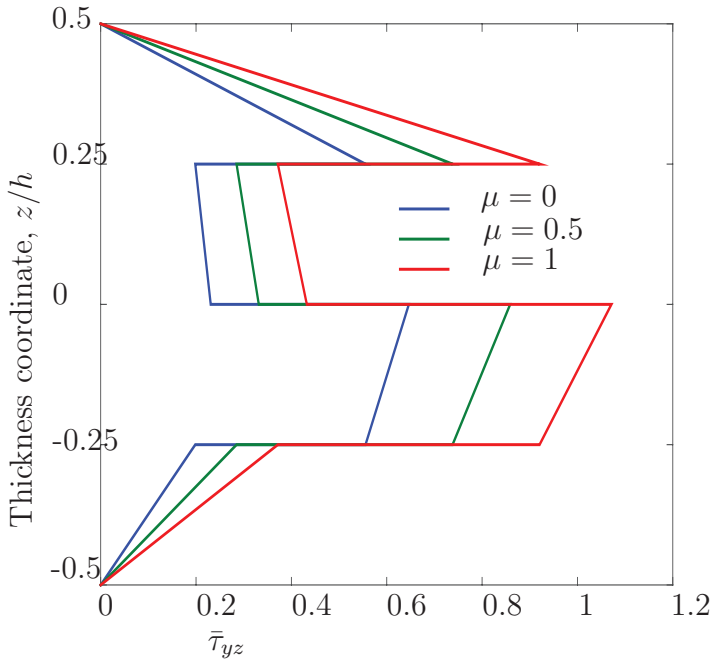

(a)

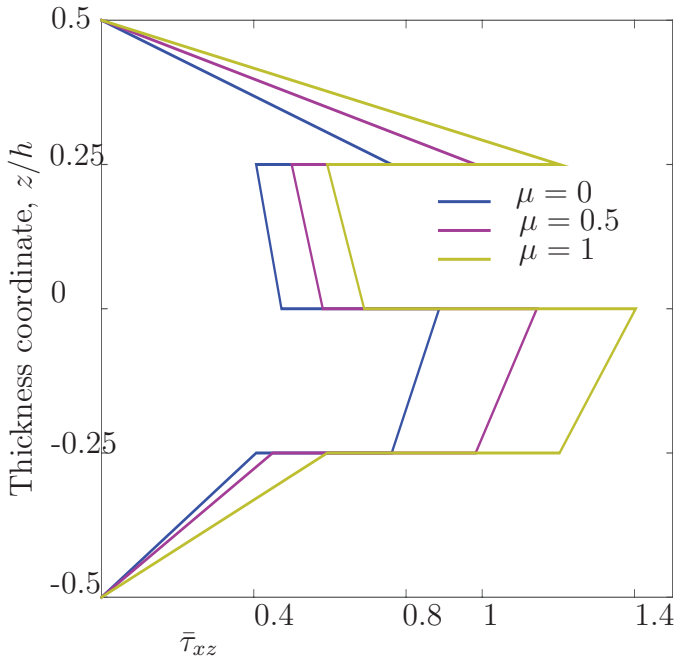

(b)

Figure 9: Distribution of shear stresses predicted by both local and nonlocal TSDT for $a/h = 10$ (a) $\bar{\tau}_{yz}$ (b) $\bar{\tau}_{xz}$

nonlocal formulation have the softening effect. Finite element models of the theory developed here can be developed to bring out the nonlocal effects on the bending and free vibration response of plates with non-rectangular geometries and boundary conditions that do not admit analytical solutions.

A Appendix

$$\begin{bmatrix} Z_{11} \\ Z_{21} \\ Z_{31} \end{bmatrix} = \begin{bmatrix} \varepsilon_{xx}^{(0)}(b+h) + \varepsilon_{xx}^{(1)} bh + \varepsilon_{xx}^{(3)}(\frac{h^4}{32} + \frac{bh^3}{4}) + \tau^s(b+h) \\ \varepsilon_{yy}^{(0)}(a+h) + \varepsilon_{yy}^{(1)} ah + \varepsilon_{yy}^{(3)}(\frac{h^4}{32} + \frac{ah^3}{4}) + \tau^s(a+h) \\ 0 \end{bmatrix} \tag{67}$$

$$\begin{Bmatrix} L_{11} \\ L_{21} \\ L_{31} \end{Bmatrix} = \begin{Bmatrix} \frac{\nu h^6 \tau^s}{6(1-\nu)} \left(\frac{\partial^2 w}{\partial x^2} + \frac{\partial^2 w}{\partial y^2} \right) + (2\mu^s + \lambda^s) \left[\varepsilon_{xx}^{(0)} bh + \varepsilon_{xx}^{(1)} \left(\frac{h^3}{12} + \frac{bh^2}{2} \right) + \varepsilon_{xx}^{(3)} \left(\frac{h^5}{80} + \frac{bh^4}{8} \right) \right] + \tau^s(b+h) \\ \frac{\nu h^6 \tau^s}{6(1-\nu)} \left(\frac{\partial^2 w}{\partial x^2} + \frac{\partial^2 w}{\partial y^2} \right) + (2\mu^s + \lambda^s) \left[\varepsilon_{yy}^{(0)} ah + \varepsilon_{yy}^{(1)} \left(\frac{h^3}{12} + \frac{ah^2}{2} \right) + \varepsilon_{yy}^{(3)} \left(\frac{h^5}{80} + \frac{ah^4}{8} \right) \right] + \tau^s(a+h) \\ 0 \end{Bmatrix} \tag{68}$$

$$\begin{Bmatrix} O_{11} \\ O_{21} \\ O_{31} \end{Bmatrix} = \begin{Bmatrix} \frac{\nu h^4 \tau^s}{40(1-\nu)} \left(\frac{\partial^2 w}{\partial x^2} + \frac{\partial^2 w}{\partial y^2} \right) + (2\mu^s + \lambda^s) \left[\varepsilon_{xx}^{(0)} \frac{bh^3}{4} + \varepsilon_{xx}^{(1)} \left(\frac{h^5}{80} + \frac{bh^4}{8} \right) + \varepsilon_{xx}^{(3)} \left(\frac{h^7}{448} + \frac{bh^6}{32} \right) \right] + \tau^s(b+h) \\ \frac{\nu h^4 \tau^s}{40(1-\nu)} \left(\frac{\partial^2 w}{\partial x^2} + \frac{\partial^2 w}{\partial y^2} \right) + (2\mu^s + \lambda^s) \left[\varepsilon_{yy}^{(0)} \frac{ah^3}{4} + \varepsilon_{yy}^{(1)} \left(\frac{h^5}{80} + \frac{ah^4}{8} \right) + \varepsilon_{yy}^{(3)} \left(\frac{h^7}{448} + \frac{ah^6}{32} \right) \right] + \tau^s(a+h) \\ 0 \end{Bmatrix} \tag{69}$$

References

[1] A.C. Eringen and D. G. B. Edelen. On nonlocal elasticity. *International Journal of Engineering Science*, 10:233–248, 1972.

[2] J. N. Reddy. *Mechanics of Laminated Composite Plates and Shells*, volume 2nd ed. CRC Press, 2004.

[3] M. E. Gurtin and I. A. Murdoch. A continuum thoery of elastic material surfaces. *Archives of Rational Mechanics and Analysis*, 57(4):291–323, 1975.

[4] M. E. Gurtin and I. Murdoch. Surface stress in solids. *International Journal for Solids and Structures*, 14:431–440, 1978.

[5] A.C. Eringen. *Microcontinuum field theories-1. Foundations and solids*. Springer- Verlag, Newyork, 1998.

[6] A. Dietsche, P. Steinmann, and K. Willam. Micropolar elastoplasticity and its role in localization analysis. *Int. J. of Plasticity*, 9:813 – 831, 1993.

[7] N. Kirchner and P. Steinmann. Mechanics of extended continua: modeling and simulation of elastic microstretch materials. *Computational Mechanics*, 40(4):651–666, 2006.

[8] E. Amanatdou and A. Aravas. On microstructural origin of certain inelastic models. *Journal of Engineering Material technology*, 106:326–330, 1984.

[9] Z. P. Bazant and M. Jirasek. Nonlocal integral formulations of plasticity and damage. *Journal of Engineering Mechanics ASCE*, 128(5-6):1119–1149, 2002.

[10] R. D. Mindlin and H. F. Tiersten. Effects of couple stress in linear elasticity. *Archive for Rational Mechanics and Analysis*, 11:415–448, 1962.

[11] R. D. Mindlin and H. F. Tiersten. Microstructure in linear elasticity. *Archive for Rational Mechanics and Analysis*, 16:51–78, 1964.

[12] R. D. Mindlin. Second gradient in strain and surface tension in linear elasticity. *International Journal of Solids and Structures*, 1(3):417–438, 1965.

[13] R. A. Toupin. Elastic materials with couple stress. *Archive for Rational Mechanics and Analysis*, 11:385–414, 1962.

[14] N. Kirchner and P. Steinmann. A micropolar theory of finite deformation and finite rotation multiplicative elastoplasticity. *Int. J. of Solids and Structures*, 31:1063 – 1084, 1994.

[15] R. Sunyk and P. Steinmann. On higher gradients in continuum atomistic modelling. *International Journal of Solids and Structures*, 40:6877–6896, 2003.

[16] N. Kirchner and P. Steinmann. On material settings of gradient hyperelasticity. *Mathematics and Mechanics of Solids*, 12(5):559–580, 2006.

[17] C. Polizzotto. Gradient elasticity and non standard boundary conditions. *International Journal for Solids and Structures*, 40:7399–7423, 2003.

[18] N. A. Fleck and J. W. Hutchinson. Strain gradient plasticity. *Adv. app.Mech*, 33, 1996.

[19] J. Y. Shu, W. E. King, and N. A. Fleck. Finite elements for materials with strain gradient effects. *International Journal for Numerical Methods in Engineering*, 44:373–391, 1999.

[20] H. Askes and E.C. Aifantis. Numerical modeling of size effects with gradient elasticity-formulation meshless discretization and examples. *International Journal of Fracture*, 117:347–358, 2002.

[21] H. Askes and M.A. Gutierrez. Implicit gradient elasticity. *International Journal of Numerical Methods in Engineering*, 67:400–416, 2006.

[22] I. Morata H. Askes, M.A. Gutierrez. Finite element analysis with staggered gradient elasticity. *Computers and Structures*, 86(1266-1279):393–496, 2008.

[23] A.C. Eringen. Balance laws of micromorphic continuua revisited. *International journal of Engineering Science*, 30(6):805–810, 1992.

[24] A.C. Eringen. Balance laws of micromorphic mechanics. *International journal of Engineering Science*, 85:819–828, 1970.

[25] A.C. Eringen. On differential equations of nonlocal elasticity and solutions of screw dislocation and surface waves. *Journal of Applied Physics*, 54:4703–4710, 1983.

[26] N. Kirchner and P. Steinmann. A unifying treatise on variational principles of gradient and micromorphic continuaa. *Philosophical Magazine*, 85(33-35):3875–3895, 2005.

[27] B. Hirschberger and P. Steinmann. On deformation and configurational mechanics of micromorphic hyperelasticity-theory and computations. *Computer Methods in Applied Mechanics and Engineering*, 40(4):4027 – 4044, 2007.

[28] M. Jirasek. Nonlocal theories in continuum mechanics. *Acta Polytechnica*, 44(5-6):16–34, 2004.

[29] M. Jirasek. Nonlocal theories in continuum mechanics. *Acta Polytechnica*, 44:5–6, 2004.

[30] J. N. Reddy. Nonlocal theories for bending, buckling and vibration of beams. *International Journal of Engineering Science*, 45:288–307, 2007.

[31] M. Aydogdu. A general nonlocal beam theory: Its application to nanobeam bending, buckling and vibration. *Physica E*, 41:1651–1655, 2009.

[32] O. Civalek and C. Demir. Bending analysis of microtubules using nonlocal euler-bernoulli beam theory. *Applied Mathematical Modelling*, 35:2053–2067, 2011.

[33] N. Ari and A. C. Eringen. Nonlocal stress field at griffith crack. *Structures and Mechanics : Report*, 54, 1980.

[34] L. Cheng, Y. Linquan, C. Weiqiu, and L. Shuang. Comments on nonlocal effects in nano-cantilever beams. *International Journal of Engineering Science*, 87:47–57, 2015.

[35] M. G. D. Geers, V. Kouznetsova, and W. A. M. Brekelmans. Gradient enhanced computational homogenization for the micro macro scale transition. *Journal of Physics*, 11(4):145–152, 2001.

[36] V. G. Kouznetsova. Computational homogenization for the multiscale analysis of multipahse materials. *PhD, thesis, Technische Universiteit, Eindhoven*, 2002.

[37] V. G. Kouznetsova, M. G. D. Geers, and W. A. M. Brekelmans. Multiscale second order computational homogenization of multiphase materials: A nested finite element solution strategy. *Computer Methods in Applied Mechanics and Engineering*, 193:5525–5550, 2004.

[38] A. R. Srinivasa and J. N. Reddy. A model for a constrained, finitely deforming, elastic solid with rotation gradient dependent strain energy, and its specialization to von karman plates and beams. *Journal of Physics and Mechanics of Solids*, 61:873–885, 2013.

[39] R. Maranganti and P. Sharma. Length scales at which classical elasticity breaks down for various materials. *Physical Review Letters*, 98:195–204, 2007.

[40] M. Aydogdu. Axial vibration of the nanorods with the nonlocal continuum rod model. *Physica E*, 41:861–864, 2009.

[41] S. Adhikari, T. Murmu, and M. A. McCarthy. Frequency domain analysis of nonlocal rods embedded in an elastic medium. *Physica E*, 59:33–40, 2014.

[42] M. Janghorban and A. Zare. Free vibration analysis of functionally graded carbon nanotubes with variable thickness by differential quadrature method. *Physica E*, 43:1602–1604, 2011.

[43] O. Civalek and B. Akgoz. Free vibration analysis of microtubules as cytoskeleton components: Nonlocal euler-bernoulli beam modeling. *Scientia Iranica*, 17:367–375, 2010.

[44] M. Hemmatnezhad. and R. Ansari. Finite element formulation for the free vibration analysis of embedded double-walled carbon nanotubes based on nonlocal timoshenko beam theory. *Journal of Theoretical and Applied Physics*, 7:6, 2013.

[45] R. Ansari and S. Sahmani. Bending behavior and buckling of nanobeams including surface stress effects corresponding to different beam theories. *International Journal of Engineering Science*, 49:1244–1255, 2011.

[46] D. Kumar, C. Heinrich, and A. M. Waas. Buckling analysis of carbon nanotubes modeled using nonlocal continuum theories. *Journal of Applied Physics*, 103:073521, 2008.

[47] S. Sahmani and R. Ansari. Nonlocal beam models for buckling of nanobeams using state-space method regarding different boundary conditions. *Journal of Mechanics, Science and Technology*, 25:2365–2375, 2011.

[48] Q. Wang, V. K. Varadan, and S. T. Quek. Small scale effect on elastic buckling of carbon nanotubes with nonlocal continuum models. *Physics Letters A*, 357:130–135, 2006.

[49] T. Murmu and S. C. Pradhan. Buckling analysis of single-walled carbon nanotubes embedded in an elastic medium based on nonlocal elasticity and timoshenko beam theory and using dqm. *Physica E*, 41:1232–1239, 2009.

[50] C. M. C. Roque, A. J. M. Ferreira, and J. N. Reddy. Analysis of timoshenko nanobeams with a nonlocal formulation and meshless method. *International Journal of Engineering Science*, 49:976–984, 2011.

[51] Q. Wang and K. M. Liewbend. Application of nonlocal continuum mechanics to static analysis of micro- and nano-structures. *Physics Letters A*, 363:236–242, 2007.

[52] C. M. Wang, Y. Y. Zhang, and X. Q. He. Vibration of nonlocal timoshenko beams. *IOP Science*, 18:105401–105410, 2007.

[53] C. M. Wang, S. Kitipornchai, C. W. Lim, and M. Eisenberg. Beam bending solutions based on nonlocal timoshenko beam theory. *Journal of Engineering Mechanics*, 134:475–481, 2008.

[54] M. Shaat. Iterative nonlocal elasticity for kirchoff plates. *International Journal of Mechanical Sciences*, 90:162–170, 2015.

[55] Huu-Tai Thai. A nonlocal beam theory for bending, buckling and vibration of nanobeams. *International Journal of Engineering Science*, 52:56–64, 2012.

[56] Huu-Tai Thai, T. P. Vo, T. K. Nguyen, and J. Lee. A nonlocal beam theory for bending, buckling and vibration of nanobeams. *International Journal of Engineering Science*, 123:337–349, 2015.

[57] S. H. Hashemi. and R. Nazemnezhad. An analytical study on the nonlinear free vibration of functionally graded nanobeams incorporating surface effects. *Composites: Part B*, 52(11):199–206, 2013.

[58] M. Zare S. H. Hashemi and R. Nazemnezhad. An exact analytical approach for free vibration of mindlin rectangular nano-plates via nonlocal elasticity. *Composite Structures*, 100:290–299, 2013.

[59] R. Lewandowski. Application of ritz method to the analysis of nonlinear vibration of beams. *Journal of Sound and Vibration*, 114:91–101, 1987.

[60] Xiao-Wen Lei, Toshiaki Natsuki, Jin xing Shi, and Qing-Qing Ni. Surface effects on the vibrational frequency of double-walled carbon nanotubes using the nonlocal timoshenko beam model. *Composites: Part B*, 43:64–69, 2012.

[61] Haw-Long Lee and Win-Jin Chang. Surface effects on frequency analysis of nanotubes using nonlocal timoshenko beam theory. *Journal of Applied Physics*, 108:093503, 2010.

[62] Shahrokh Hosseini-Hashemi, Reza Nazemnezhad, and Hossein Rokni. Nonlocal nonlinear free vibration of nanobeams with surface effects. *European Journal of Mechanics A/Solids*, 52:44–53, 2015.

[63] S. P. Xu. An operational calculus-based approach to a general bending theory of nonlocal elastic beams. *European Journal of Mechanics A/Solids*, 46:54–59, 2014.

[64] F. M. deSciarra. Finite element modelling of nonlocal beams. *Physica E*, 59:144–149, 2014.

[65] C. T. Sun and H. Zhang. Size dependent elastic moduli of plate like nanomaterials. *Journal of Applied Physics*, 93:1212–1218, 2003.

[66] T. Murmu and S. C. Pradhan. Thermo-mechanical vibration of single-walled carbon nanotube embedded in an elastic medium based on nonlocal elasticity theory. *Computational Material Science*, 46:854–859, 2009.

[67] O. Rahmani and O. Pedram. Analysis and modeling the size effect on vibration of functionally graded nanobeams based on nonlocal timoshenko beam theory. *International Journal of Engineering Science*, 77:55–70, 2014.

[68] G. Yun and H. S. Park. Surface stress effects on the bending properties of FCC metal nanowires. *Physical Review : B*, 195:421–423, 2009.

[69] G. Borino and C. Polizzotto. A method to transform a nonlocal model in to a gradient one within elasticity and plasticity. *European Journal of Mechanics A/ Solids*, 46:30–41, 2014.

[70] H. Niknam and M. M. Aghdam. A semianalytical approach for large amplitude free vibration and buckling of nonlocal FG beams on elastic foundation. *Composite Structures*, 119:452–462, 2015.

[71] R. Barretta and F. M. de Sciarra. A nonlocal model for carbon nano tubes under axial loads. *Advances in Material Science and Engineering*, 2013:1–6, 2013.

[72] R. Aghababaei and J.N. Reddy. Non local third order shear deformation theory with application to bending and vibration of plates. *International Journal of Engineering Science*, 326:277–289, 2009.

[73] A. Bhar, S.S. Phoenix, and S.K. Satsangi. Finite element analysis of laminated composite stiffened plates using fsdt and hsdt: A comparative perspective. *Composite Structures*, 92:312–321, 2010.

[74] M. Cetkovic and Dj. Vuksanovic. Bending, free vibrations and buckling of laminated composite and sandwich plates using a layer wise displacement model. *Composite Structures*, 88:219–227, 2009.

[75] M. Cetkovic and Dj. Vuksanovic. A generalized high-order globallocal plate theory for nonlinear bending and buckling analyses of imperfect sandwich plates subjected to thermo-mechanical loads. *Composite Structures*, 92:130–143, 2010.

[76] S. Xianga, S. Jiangb, Z. Bic, Yao xing Jind, and M. Yanga. A nth-order meshless generalization of reddys third-order shear deformation theory for the free vibration on laminated composite plates. *Composite Structures*, 93:299–307, 2011.

[77] J. N. Reddy and E. J. Barbero. A plate bending element based on generalized laminate theory. *International Journal for Numerical Methods in Engineering*, 28:2275–2292, 1989.

[78] T. Kant and K. Swaminathan. Mechanics of laminated composite plates theory and analysis. *Composite Structures*, 56:329–344, 2002.

[79] D. Wang and A. I. E. I. Sheikh. Large deflection mathematical analysis of plates. *Journal of Engineering Mechanics*, 131:809–821, 2005.

[80] P. Lu, P. Q. Zhang, H. P. Lee, C. M. Wang, and J. N. Reddy. Non-local elastic plate theories. *Proceedings of the Royal society*, 463:3225–3240, 2007.

[81] A. Farajpour, A. R. Shahidi, M. Mohammadi, and M. Mahzoon. Buckling of orthotropic micro/nano scale plates under linearly varying in-plane load via nonlocal continuum mechanics. *Composite Structures*, 94:1605–1615, 2012.

[82] A. M. A. Neves, A. J. M. Ferreira, E. Carrera, M. Cinefra, C.M.C. Roque, R. M. N. Jorge, and C. M. M. Soares. Static, free vibration and buckling analysis of isotropic and sandwich functionally graded plates using a quasi-3d higher-order shear deformation theory and a meshless technique. *Composites : Part B*, 44:657–674, 2013.

[83] B. Arash and Q. Wang. A review on the application of nonlocal elastic models in modeling of carbon nano tubes and graphenes. *Computational Materials Science*, 51:303–313, 2012.

[84] J.W. Yan, L. H. Tong, C. Li, Y. Zhu, and Z. W. Wang. Exact solutions of bending deflections for nano-beams and nano-plates based on nonlocal elasticity theory. *Composite Structures*, 125:304–313, 2015.

[85] C. M. Wang, Y. Y. Zhang, S. S. Ramesh, and S. Kitipornchai. Buckling analysis of micro- and nano-rods/tubes based on nonlocal timoshenko beam theory. *Journal of Physics*, 39:3904–3909, 2006.

[86] T. Murmu and S. Adhikari. Nonlocal transverse vibration of double-nanobeam-systems. *Journal of Applied Physics*, 108(8):083514, 2010.

[87] C. Y. Wang, T. Murmu, and S. Adhikari. Mechanisms of nonlocal effect on the vibration of nano plates. *Applied Physics Letters*, 98:153101, 2011.

[88] S.C. Pradhan and T. Murmu. Small scale effect on the buckling of single-layered graphene sheets under biaxial compression via nonlocal continuum mechanics. *Computational Materials Science*, 47:268–274, 2007.

[89] T. Murmu and S. C. Pradhan. Small-scale effect on the free in-plane vibration of nano plates by nonlocal continuum model. *Physica*, 41:1628–1633, 2009.

[90] T. Murmu and S. C. Pradhan. Small scale effect on the buckling analysis of single-layered graphene sheet embedded in an elastic medium based on nonlocal plate theory. *Physica*, 42:1293–1301, 2010.

[91] C. S. Han. Influence of the molecular structure on indentation size effect in polymers. *Materials Science and Engineering*, 527:619–624, 2010.

[92] S. Nikolov, C. S. Han, and D. Raabe. On the origin of size effects in small-strain elasticity of solid polymers. *International Journal of Solids and Structures*, 44:1582–1592, 2007.

[93] J. N. Reddy. A refined nonlinear theory of plates with transverse shear deformation. *International Journal of Solids and Structures*, 20(9-10):881–896, 1984.